AD NUMBER

ADB000591

LIMITATION CHANGES

TO:

Approved for public release; distribution is unlimited.

FROM:

Distribution authorized to U.S. Gov't. agencies only; Test and Evaluation; MAY 1974. Other requests shall be referred to Air Force Materials Laboratory, AFML/MBC, Wright-Patterson AFB, OH 45433.

AUTHORITY

afwal ltr, 21 sep 1982

AFML-TR-73-147
Part II

GRAPHITE FIBERS FROM PITCH

R. DIDCHENKO,
PRINCIPAL INVESTIGATOR
UNION CARBIDE CORPORATION
CLEVELAND, OHIO

TECHNICAL REPORT AFML—TR—73—147, PART II

MARCH 1974

AIR FORCE MATERIALS LABORATORY
AIR FORCE SYSTEMS COMMAND
WRIGHT—PATTERSON AIR FORCE BASE, OHIO 45433

NOTICES

When Government drawings, specifications, or other data are used for any purpose other than in connection with a definitely related Government procurement operation, the United States Government thereby incurs no responsibility nor any obligation whatsoever; and the fact that the Government may have formulated, furnished, or in any way supplied the said drawings, specifications, or other data, is not to be regarded by implication or otherwise as in any manner licensing the holder or any other person or corporation, or conveying any rights or permission to manufacture, use, or sell any patented invention that may in any way be related thereto.

This report has been reviewed and is approved for publication.

Theodore J. Reinhart Jr

For the Commander:

Copies of this report should not be returned unless return is required by security considerations, contractual obligations, or notice on a specific document.

AIR FORCE/56780/13 December 1974 — 350

SECURITY CLASSIFICATION OF THIS PAGE (When Data Entered)

REPORT DOCUMENTATION PAGE		READ INSTRUCTIONS BEFORE COMPLETING FORM
1. REPORT NUMBER AFML-TR-73-147	2. GOVT ACCESSION NO.	3. RECIPIENT'S CATALOG NUMBER
4. TITLE (and Subtitle) GRAPHITE FIBERS FROM PITCH		5. TYPE OF REPORT & PERIOD COVERED Technical Report - Part II Feb. 1973 - Jan. 1974 6. PERFORMING ORG. REPORT NUMBER
7. AUTHOR(s) R. Didchenko, Principal Investigator		8. CONTRACT OR GRANT NUMBER(s) F33615-71-C-1538
9. PERFORMING ORGANIZATION NAME AND ADDRESS Union Carbide Corporation P. O. Box 6116 Cleveland, Ohio 44101		10. PROGRAM ELEMENT, PROJECT, TASK AREA & WORK UNIT NUMBERS 62101, 7320, 73200135
11. CONTROLLING OFFICE NAME AND ADDRESS DCASR-Cleveland, Federal Office Building 1240 E. 9th Street Cleveland, Ohio 44114		12. REPORT DATE March, 1974 13. NUMBER OF PAGES 74
14. MONITORING AGENCY NAME & ADDRESS (if different from Controlling Office) Air Force Materials Laboratory AFML/MBC Wright-Patterson AFB, Ohio 45433		15. SECURITY CLASS. (of this report) Unclassified 15A. DECLASSIFICATION/DOWNGRADING SCHEDULE NA

16. DISTRIBUTION STATEMENT (of this Report)

Distribution limited to U. S. Government Agencies only.

17. DISTRIBUTION STATEMENT (of the abstract entered in Block 20, if different from Report)

Same as Report

18. SUPPLEMENTARY NOTES

None

19. KEY WORDS (Continue on reverse side if necessary and identify by block number)

CARBON
FIBERS
GRAPHITE
PITCH

20. ABSTRACT (Continue on reverse side if necessary and identify by block number)

Methods to measure molecular weight distributions in MP pitches have been developed. Number and weight average molecular weights and their distributions have been determined as a function of P. I. in MP pitches.

Significant progress has been achieved during this report period both in the art of spinning very thin MP pitch filaments and in the understanding of structural changes that take place during the conversion of pitch fibers to high-performance carbon fibers.

The properties of the carbonized monofilament in some instances exceeded

DD FORM 1 JAN 73 1473 EDITION OF 1 NOV 65 IS OBSOLETE

SECURITY CLASSIFICATION OF THIS PAGE (When Data Entered)

20. the target properties. Elongations to break between 1.2 and 1.9 percent have been repeatedly observed in filaments with short gauge tensile strengths ranging from 2.75 to 3.45 GPa (400 x 10^3 psi to 500 x 10^3 psi). The highest average monofilament values were: 3.45 GPa (510 x 10^3 psi) long gauge tensile strength; 4.14 GPa (600 x 10^3 psi) short gauge tensile strength; 440 GPa (64 x 10^6 psi) elastic modulus. The properties of continuously processed multifilament yarn were lower but have attained already useful levels, viz., strand tensile strength of 1.77 GPa (256 x 10^3 psi), elastic modulus of 228 GPa (33 x 10^6 psi), and elongation-to-break of 0.8 percent.

PREFACE

The work reported herein was performed under the sponsorship of the Air Force Systems Command, United States Air Force, Wright-Patterson Air Force Base, Ohio 45433, Contract No. F33615-71-C-1538, Project No. 7320, Fibrous Materials for Decelerators and Structures, Task No. 732001, Organic and Inorganic Fibers. The technical direction was provided by Mr. W. H. Gloor, Project Engineer, Composite and Fibrous Materials Branch, Nonmetallic Division, AFML.

The Contract is Union Carbide Corporation, Carbon Products Division, Parma Technical Center, P. O. Box 6116, Cleveland, Ohio 44101.

The Senior Investigator is Dr. R. Didchenko. Major contributors to the effort are Dr. J. B. Barr, Dr. S. Chwastiak, Dr. I. C. Lewis, Dr. R. T. Lewis, and Dr. L. S. Singer. They are assisted by Mrs. Barbara Petro (GPC), Messrs. J. D. Ruggiero and A. F. Silvaggi, Jr. (Microscopy) and by the Fiber Testing Group under Dr. D. J. Kampe. Dr. S. L. Strong helped and consulted in the X-ray Studies.

This report covers the period from February 1973 to January 1974.

TABLE OF CONTENTS

TABLE OF CONTENTS (Cont'd)

LIST OF ILLUSTRATIONS

LIST OF ILLUSTRATIONS (Cont'd)

LIST OF TABLES

SECTION I

INTRODUCTION

This Technical Report contains the results of the continuing effort under Contract No. F33615-71-C-1538. The goal of the Contract is to demonstrate the feasibility of an economic, continuous process for high-performance carbon/graphite fibers from pitch. The target for the tensile strength of the fibers was set at 2.75 GPa (400 x 10^3 psi) with a minimum elongation-to-break of 0.8 percent.

In Part I of this report series (AFML-TR-73-147, June 1973) the preparation and the rheological properties of suitably modified pitches were described along with some very promising properties obtained on monofilaments of carbon fibers derived from these pitches. The effort in the period covered in this report was expended on achieving a better understanding of the molecular weight distribution of spinnable pitches; on spinning and processing ultrafine (< 10μm diameter) monofilament; and on continuous processing of multifilament yarn. The investigation of fiber structure and its correlation with fiber properties also has been initiated. All these studies led to significant improvements in both the processing and the properties of the fibers. The target properties have been repeatedly exceeded in carbon monofilaments.

SECTION II

SUMMARY

Methods have been developed to study the molecular weight distribution in the MP pitches by Gel Permeation Chromatography. The molecular weight distributions in both the P.S. fraction and in the toluene soluble portion of the reduced P.I. fraction were redetermined as a function of the P.I. content of MP pitch. The results show that the large molecular species are most reactive in producing the P.I. fraction. Monofilaments with diameters from 7.5μm to 10μm have been spun consistently on the improved spinning apparatus.

After carbonization and final heat-treatment at 1650°C, these monofilaments had diameters ranging from about 5 to 7μm. The average short gauge tensile strength of individual batches was often in excess of 2.75 GPa (400×10^3 psi) while their elastic moduli varied from 240 GPa (35×10^6 psi) to 440 GPa (64×10^6 psi). The highest average properties of a batch of monofilaments were: 3.45 GPa (510×10^3 psi), long gauge tensile strength; 4.14 GPa (600×10^3 psi), short gauge tensile strength; 440 GPa (64×10^6 psi), elastic modulus. An elongation-to-break of 1.6 percent was obtained in a sample which had short gauge tensile strength of 4.00 GPa (580×10^3 psi) and a Young's modulus of 255 GPa (37×10^6 psi). An even higher elongation-to-break (1.9 percent) was reached in a sample with an elastic modulus of 200 GPa (29×10^6 psi).

In continuous processing of a 120 filament yarn, the best strand properties achieved after final heat-treatment at 1650°C were 1.74 GPa (252×10^3 psi) tensile strength and 276 GPa (40×10^6 psi) elastic modulus. A better combination of properties was obtained in a 240 filament yarn which had a strand tensile strength of 1.77 GPa (256×10^3 psi) and an elastic modulus of 228 GPa (33×10^6 psi), reflecting an elongation-to-break of 0.8 percent. Thermosetting of pitch fibers with nitrogen dioxide was investigated and abandoned for reasons of experimental difficulties and hazards.

A study has been initiated to correlate the fiber structure with fiber properties. Preliminary results show that not only the external filament geometry but also certain elements of the internal structure must be preserved in the thermosetting step. The crystalline stack height and the degree of preferred orientation of the thermoset fibers decrease slightly during carbonization up to 1000°C but then increase significantly upon further heat-treatment.

The torsional shear strength of 1650°C fibers in an epoxy composite was increased by surface treatment from about 32.7 MPa (4750 psi) to 89.0 MPa (12,900 psi).

SECTION III

MOLECULAR WEIGHT DISTRIBUTION IN MP PITCHES

It has been found in our studies[1] that when the same P.I. content of an MP pitch has been achieved under different preparation conditions, the pitches often showed considerable variations in their rheological and spinning behavior. These variations which are attributed to differences in the molecular weight distributions, ultimately are reflected in the uniformity, structure, and processibility of the fibers. It was, therefore, deemed justified to develop methods to measure the molecular weight distributions in the MP pitches.

1. Analytical Methods

The Gel Permeation Chromatography (GPC) technique has been selected as the most promising method for determining the molecular weight distribution in MP pitches. Although GPC has been employed extensively for polymers, its application to pitches presents some unique difficulties:

> The molecular weight range involved is very low (about 500 to 3500) compared to more conventional polymer systems.
>
> The MP pitches are very insoluble.
>
> The use of model compounds for calibration is not feasible because the separation of aromatics is based on complex factors of shape and size as well as on molecular weight.[2] These difficulties were alleviated by several modifications of the standard GPC procedures.

To encompass the low molecular size range, a column set was used, which included four columns of the lowest pore size available. The pore sizes of the columns ranged from about 45nm to 250nm as contrasted to the range of 10^3nm to 10^6nm employed in conventional polymer analysis. Toluene at 80°C was used as a solvent system after other solvents had been eliminated as unsuitable. The samples were stirred with hot toluene and filtered. An estimated 50 to 60 percent of the P.S. fraction of MP pitches was extracted by this procedure. Fortunately, the limited solubility in toluene does not produce a fractionation of molecular weights since the average molecular weights of toluene solubles and of pyridine soluble fractions, as measured by osmometry, are nearly identical.

In order to obtain GPC data for the P.I. portion of MP pitch, a prior reduction with lithium and ethylene diamine is required to render this material soluble in toluene. This reduction procedure has been described in the previous report.[3]

2. Calibration of the GPC Apparatus

The Waters GPC instrument was first calibrated for molecular size. Narrow fractions of polystyrene and polyglycol (supplied by Waters Assoc.) were used to relate elution volume to chain length in nanometers. Linear alkanes were used to extend the calibration to smaller chain lengths. A smooth curve was drawn through the semilog plot of the chain length versus the elution volume (counts). Figure 1 shows the calibration curve obtained for the elution volume range of an MP pitch.

Figure 2 shows the manner in which the molecular size distribution data can be plotted for a typical MP pitch. The plots show the cumulative percent of material as a function of molecular size for toluene soluble portions of the P.S. and reduced P.I. fractions. It is of interest that the P.S. fraction shows a very narrow distribution in molecular size, while the distribution in the P.I. fraction is quite broad. The size range of 4 to about 12nm in the P.S. fraction corresponds to about 4 to 10 condensed aromatic rings. The broad size distribution of the P.I. fraction indicates that the polymerization process leads to dimers, trimers, and even tetramers of the reactant molecules of the P.S. fraction.

3. Molecular Size Data for MP Pitch

Table I presents molecular size distribution data for a precursor petroleum pitch and for the P.S. and the reduced P.I. fractions of an MP pitch derived from it. The data are presented in terms of weight average molecular size in nanometers ($\overline{A}w$), the number average molecular size in nanometers ($\overline{A}n$), and a molecular size distribution parameter, ($D = \overline{A}w/\overline{A}n$). The precision of the $\overline{A}w$ and $\overline{A}n$ measurements is about ±0.15 while the precision in the D values is ±0.010.

TABLE I

MOLECULAR SIZE DATA FOR MP PITCH

Material	$\overline{A}w$, in nm	$\overline{A}n$, in nm	$D(\overline{A}w/\overline{A}n)$
Precursor Petroleum Pitch (175°C S.P.)	0.86	0.63	1.367
P.S. Fraction of MP Pitch	0.65	0.51	1.264
Reduced P.I. Fraction of MP Pitch	5.79	4.17	1.390

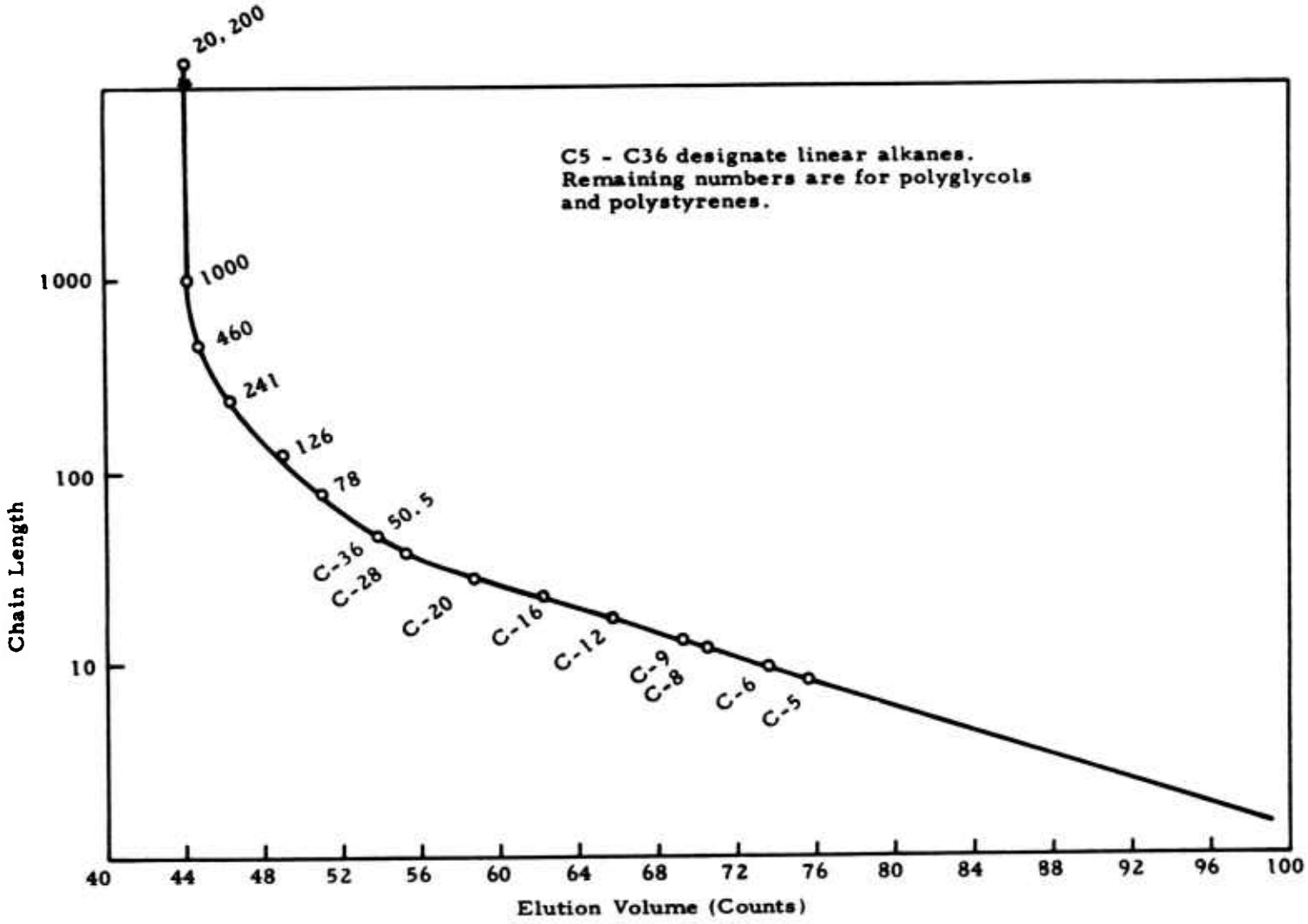

Figure 1. GPC Calibration Plot of Elution Volume vs Chain Length

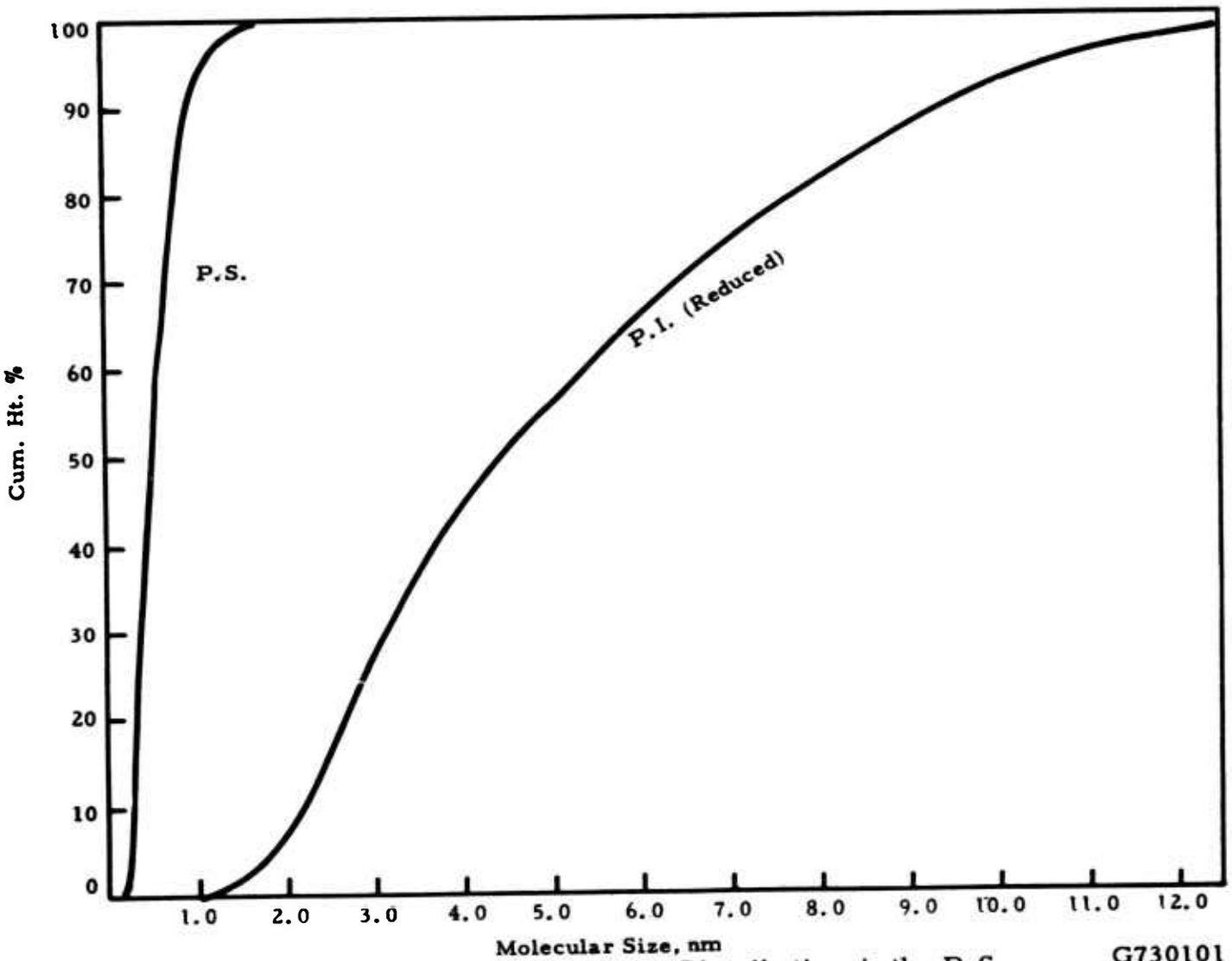

Figure 2. Molecular Size Distributions in the P.S. and P.I. Fractions of MP Pitch

The data in Table I show that both the distribution parameter, D, and the average molecular size for the P.S. decreases with P.I. formation. This result suggests that the larger molecules of the precursor pitch are the most reactive. Both the size distribution parameter and the average molecular size of the reduced P.I. fraction are considerably greater than those of the P.S. fraction.

4. Calibration of the GPC for Molecular Weight

In order to obtain molecular weight distribution data for MP pitch, the GPC apparatus was recalibrated in terms of molecular weight. Selected fractions of MP pitch were used as standards. Results based on such calibration should be much more meaningful for pitches than those based on polystyrene polymers. The following procedure was employed in the calibration.

A 10 gram sample of standard MP pitch was separated into its individual P.S. and P.I. fractions.

The P.I. fraction was reduced with lithium in ethylene diamine to produce a solubilized product.

Three successive GPC runs were made on each of the P.S. and reduced P.I. materials; the chromatographic fractions were then collected from each run and the identical ones were combined. In this manner about 50 fractions were collected for both the P.S. and for the reduced P.I. materials.

Fifteen selected GPC fractions of the P.S. materials and 15 fractions of the reduced P.I. materials were subjected to molecular weight measurement by vapor phase osmometry.

These molecular weight data were plotted versus elution volume to give the calibration curve shown in Figure 3. The curve was determined by a least squares analysis of the data.

It is apparent that the molecular weight composition of MP pitch ranges from about 500 to 3500. The higher molecular weight components of the P.S. fraction show molecular weights in the range of 1000 or greater which overlaps the molecular weights of the species in the P.I. fraction.

Table II presents molecular weight data for a precursor and an MP pitch obtained with this GPC calibration curve. The results include the weight average molecular weight ($\overline{M}w$), the number average molecular weight ($\overline{M}n$), and the molecular weight distribution parameter ($D = \overline{M}w/\overline{M}n$).

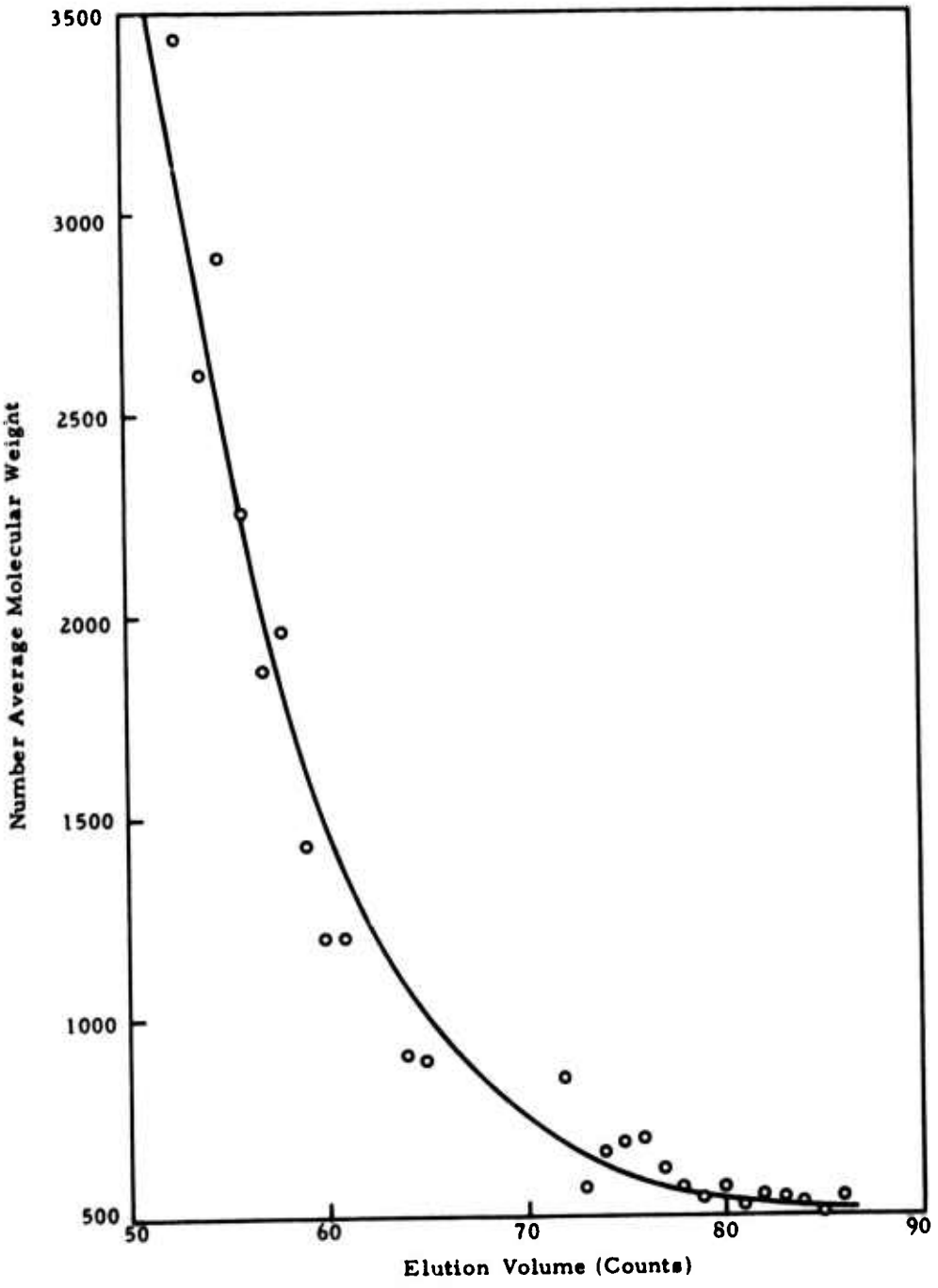

Figure 3. Calibration Curve of Number Average Molecular Weight vs Elution Volume for a Typical MP Pitch

G730103

TABLE II

MOLECULAR WEIGHT DATA FOR MP PITCH

Material	$\overline{M}w$	$\overline{M}n$	$D(\overline{M}w/\overline{M}n)$
Precursor Petroleum Pitch	674	629	1.071
P.S. Fraction of MP Pitch	592	582	1.017
Reduced P.I. Fraction of MP Pitch	2800	2330	1.203

Comparison of the P.S. material with the precursor pitch shows the same trend as that found for molecular size; both the average molecular weight and molecular weight distribution parameter decrease with increasing P.I. formation.

The molecular weight value for the reduced P.I. fraction in Table II is about four times that of the P.S. This result leaves little doubt that the formation of MP pitch involves a thermal polymerization process.

5. Effect of P.I. Content on the Molecular Weight Distribution of MP Pitch

Table III lists the molecular weight data for the toluene solubles of both the P.S. and the reduced P.I. fractions of a variety of MP pitches prepared at the same temperature but having different P.I. contents. The amount of the reduced P.I., which has resisted solubilization, is listed in the last column of the table.

A general decrease in both the molecular weight averages and the distribution parameter D with increasing P.I. formation is seen for the P.S. fraction. The decrease in the molecular weight distribution in the P.S. fraction with increasing reaction is to be expected. As more of the molecular components of the P.S. fraction react, the overall distribution narrows. The concurrent decrease in the molecular weight average implies again that the larger constituents of the P.S. fraction polymerize most easily to form P.I.

Figure 4 presents a plot of D value for the P.S. fraction versus P.I. content in the starting MP pitch. The curve shows that the D value reaches unity at a 100 percent P.I.

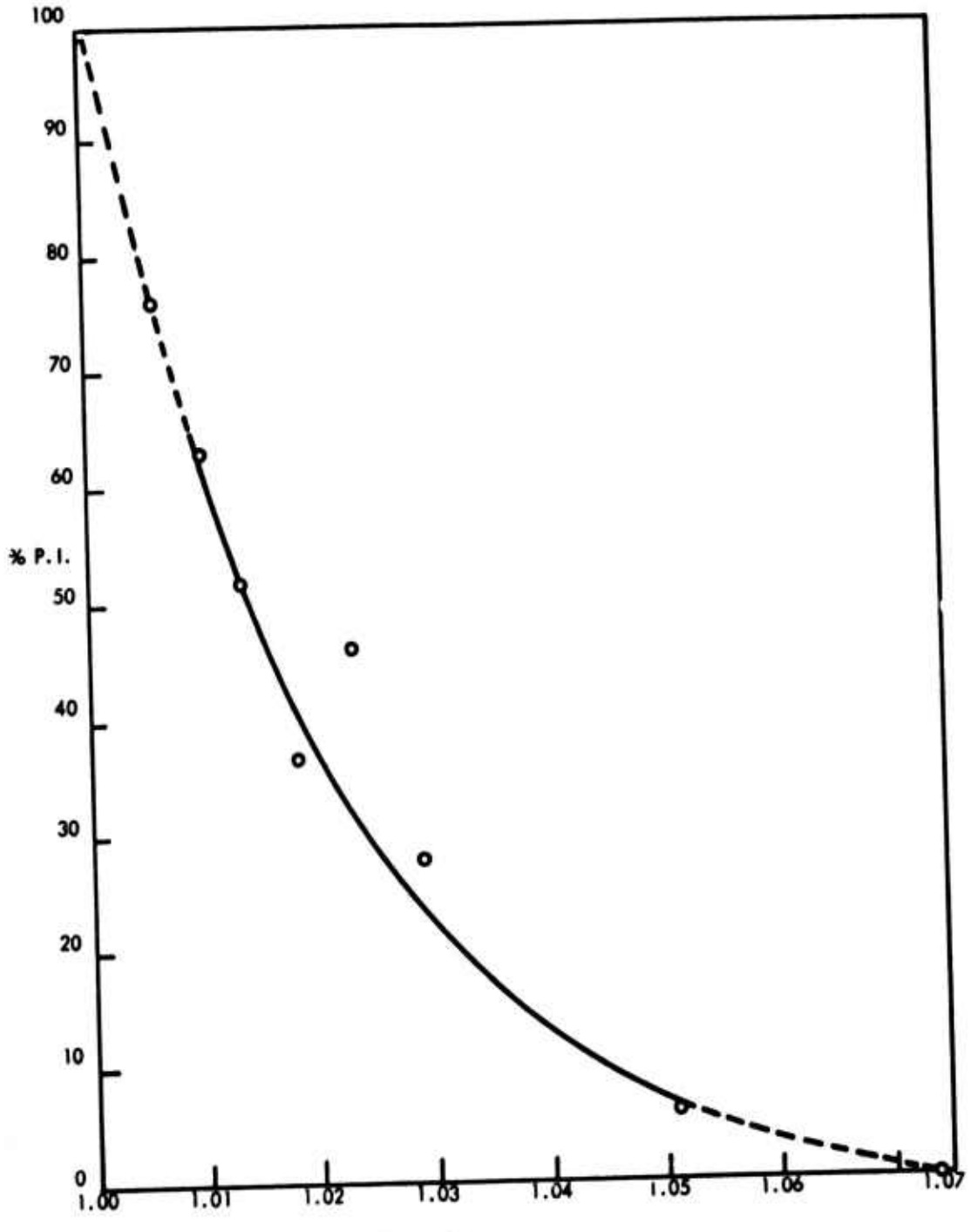

Figure 4. Plot of Percent P.I. in MP Pitch vs D Value of the P.S. Fraction

G730271

TABLE III

MOLECULAR WEIGHT DATA FOR MP PITCH
AS A FUNCTION OF P.I. CONTENT

MP Pitch % P.I.	P.S. $\overline{M}n$	P.S. $\overline{M}w$	P.S. D	Reduced P.I. $\overline{M}n$	Reduced P.I. $\overline{M}w$	Reduced P.I. D	Reduced P.I. % undissolved
~ 0[a]	640	687	1.074	----	----	-----	---
6	613	644	1.051	----	----	-----	---
28	597	614	1.029	2220	2740	1.233	3.4
37	582	593	1.018	2270	2700	1.192	0.8
46	586	600	1.018	1840	2230	1.209	2.5
52	579	586	1.013	2250	2740	1.215	0.7
63	571	576	1.010	2090	2540	1.215	1.0
76	569	566	1.006	2230	2750	1.271	46.2

[a]Precursor petroleum pitch (175°C S.P.).

Figure 5 shows a similar plot of the P.I. content versus the average molecular weights $\overline{M}w$ and $\overline{M}n$ of the P.S. fractions. Both molecular weights decrease and the curves approach each other at high P.I. contents.

Let us now consider the results for the P.I. fractions presented in Table III. It is apparent that the average molecular weights for the reduced P.I. are about three times higher than those of the P.S. The considerably higher D values for the P.I. indicate a much broader distribution of molecular weights, consistent with a polymerization mechanism. The most significant parameter for the reduced P.I. is the amount insoluble after reduction with lithium. Only the high P.I. pitch (76 percent) contains a large amount of this undissolved material. This result indicates that at high P.I. levels the molecular components of the P.I. fraction continue to react with each other.

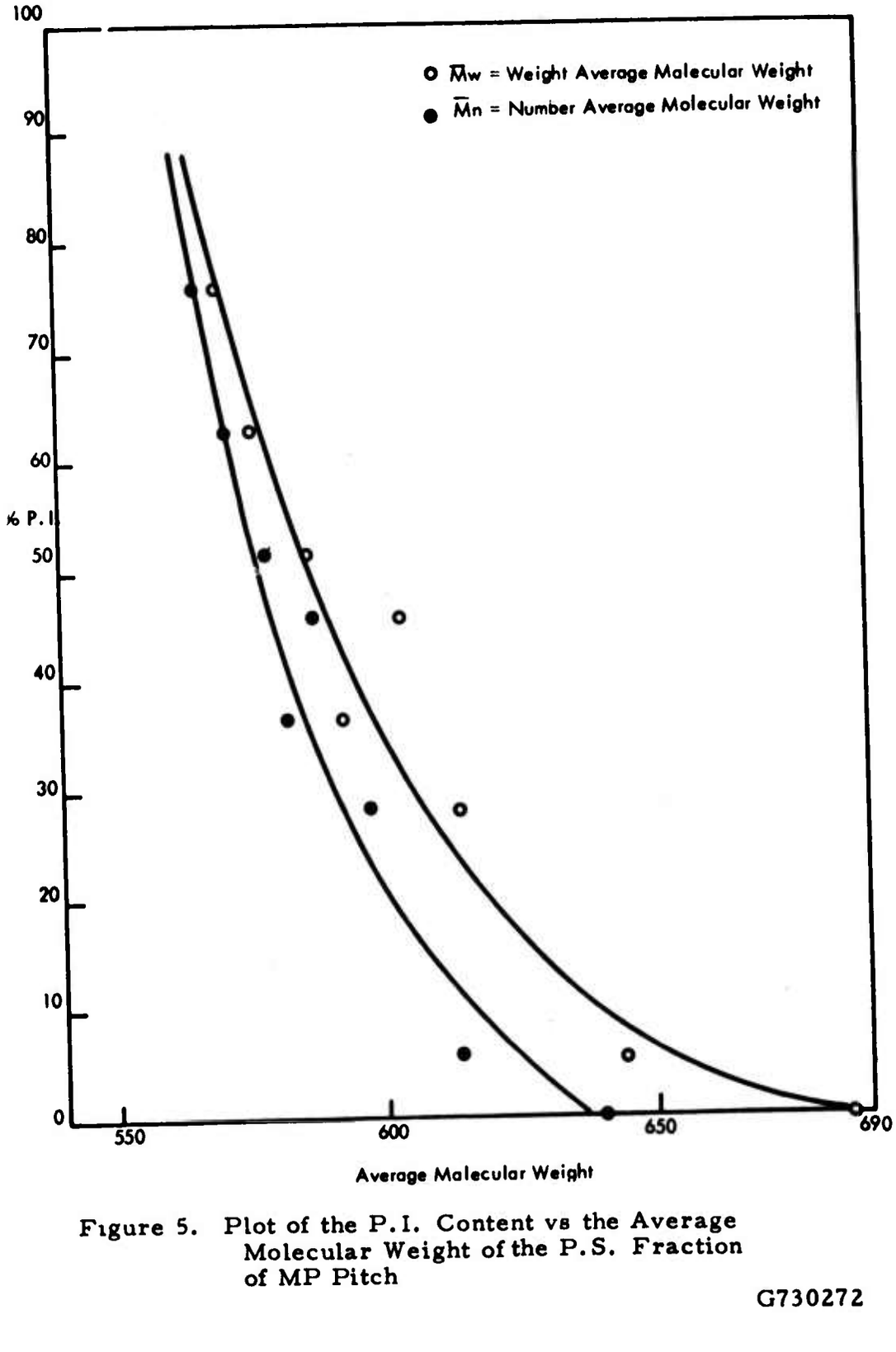

Figure 5. Plot of the P.I. Content vs the Average Molecular Weight of the P.S. Fraction of MP Pitch

G730272

SECTION IV

SPINNING

The problems of spinning fine filaments and of obtaining uniform structure are interrelated. It was easier to obtain both fine filaments and uniform textures from the well-spinning pitches which became available recently. Some evidence of structural nonuniformity was still seen occasionally, even with these good pitches, so it was decided to stir the pitch in the pot of the monofilament apparatus. This required a complete redesign of the apparatus, including the spinnerette. In the first design, the stirrer was located near the bottom of the pot but a relatively large dead volume still existed above the spinnerette. In the improved design, the dead volume was eliminated by extending the stirrer shaft into the spinnerette to within a few millimeters of the orifice. The details of the construction of the monofilament spinning head are shown in Figure 6. Pitch filaments spun with the improved apparatus had much more uniform texture.

Cartridge heaters were mounted in the spinnerette body insulated with a transite cover. The temperature of the spinnerette, monitored with a fine thermocouple, was then controlled to within 2°C of the pitch temperature. The present spinnerettes are machined out of aluminum which, being a good heat conductor, results in a uniform temperature distribution. However, the orifice quality is poor compared to the standards of commercially drilled orifices in stainless steel spinnerettes. It was expected that the smoothness and uniformity of commercial spinnerette holes might contribute to the ease of spinning and to improvement in the quality of filaments obtained. Attempts to use commercial stainless steel spinnerette discs with 4 and 5 holes were unsuccessful. Even if all the holes but one were sealed, these spinnerettes did not work. A single hole spinnerette with an aluminum body was made by mounting in it a small disc containing the hole from a commercial stainless steel spinnerette. These spinnerettes performed reasonably well, presumably because of the improved thermal conductivity, but they were still inferior to the all-aluminum spinnerettes.

The monofilament spinning machine was further improved by replacing the Leesona winder with the smoother operating Meteor coil winder. The filaments were collected in discrete bands on cardboard spools. Filaments as fine as 7.5μm diameter have been spun repeatedly with this apparatus.

Three types of structures have been observed in the as-spun fibers: radial, onionskin, and random. A detailed description of these structures is given in Section VIII. Most filaments in the yarn, spun as described in the previous report,[1] have a radial orientation but some exhibit random structure.

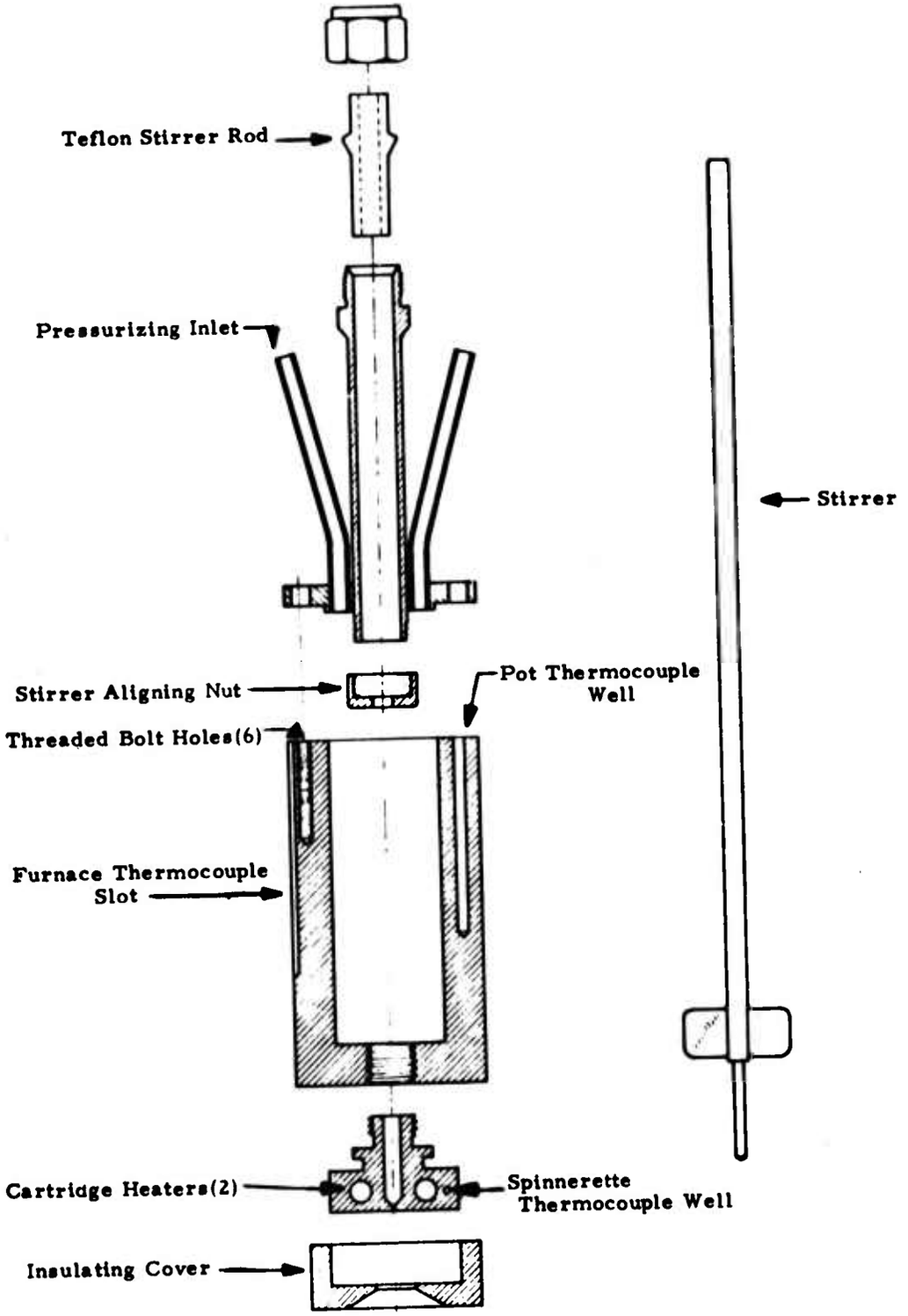

Figure 6. Monofilament Spinning Head

G740096

The monofilament machine produced mostly the random structure, with occasional occurrence of an onionskin structure. We have not yet succeeded in identifying which elements of the spinning process are responsible for these structural variations.

SECTION V

PROCESSING OF YARN

1. Development of Continuous Line

The continuous processing line, described in the previous report, was redesigned. The movable belt, used for thermosetting, was replaced by a liquid bath and a gas phase oxidation furnace. The liquid removes the yarn finish and renders infusible the filament surface. The partial infusibilization by the liquid bath allows the fiber to be heated in the oxidation furnace without melting or deforming at temperatures favorable for rapid reaction with oxygen.

Initially, the thermoset fibers were processed continuously up to 1000°C, collected on spools, and then heat-treated to 1600°-1700°C in a separate furnace. Fibers prepared by this method exhibited properties matching those of small samples processed in batches through identical stages. For example, batch processing of multifilament (15μm diameter) pitch fiber yielded a carbonized product with a short gauge (3 mm) tensile strength of 1.60 GPa (232×10^3 psi) and with a Young's modulus of 241 GPa (35×10^6 psi). Careful matching of the continuous process to the batch processing conditions produced, in two separate runs, fibers with average short gauge tensile strength between 1.59 GPa (231×10^3 psi) and 1.45 GPa (210×10^3 psi) and with Young's modulus between 179 GPa (26×10^6 psi) and 193 GPa (28×10^6 psi).

The strength of the carbonized fiber is sensitive to the thermosetting conditions. In experiments in which only the temperature of the second stage was increased, the average short gauge tensile strengths decreased from 1.54 GPa (203×10^3 psi) to 0.89 GPa (129×10^3 psi).

The thermoset yarn was weak and brittle, but its handleability improved after heating it at 1000°C. The continuous line was operated at a rate of only 20 meters per hour to minimize the damage to the yarn by transport rollers and flexing devices.

Single filament properties representative of the better yarn samples prepared at this stage of our work are listed in Table IV. Large differences between average and maximum tensile strengths demonstrate lack of uniformity through the fiber bundle. Long gauge average values were often as low as 0.69 GPa (100×10^3 psi), while the maximum short gauge values fell sometimes in the range of 2.75 GPa (400×10^3 psi) to 3.45 GPa (500×10^3 psi).

Strand testing of epoxy impregnated yarn was introduced as larger amounts of carbonized fibers became available. The strand fiber tests were carried out with 25 mm gauge lengths for tensile strength measurements (10 strands) and 125 mm gauge lengths (2 strands) for the Young's modulus.

TABLE IV

CARBON FIBER SINGLE FILAMENT PROPERTIES

Run No.	Short Gauge Tensile Strength Average GPa	Average (10^3 psi)	Maximum GPa	Maximum (10^3 psi)	Average Young's Modulus GPa	Average Young's Modulus (10^6 psi)	Avg. Break Strain (%)
6-89A	1.54	223	2.68	389	234	34	0.62
6-95A	1.77	256	3.21	466	200	29	0.89
6-100A	1.81	262	3.68	534	200	29	0.90
11-1A	1.46	212	2.34	339	235	34	0.51

The strand data are generally believed to be more indicative of composite properties than are the single filament data. Strand tensile strengths averaging 1.55 GPa (225 x 10^3 psi) and higher were common but they were generally lower than the single filament properties. The average diameters of carbonized filaments were approximately 11μm; the densities of the 1650°C carbonized products were about 2.0 Mg/m^3. Table V shows strand data for some of the better yarn samples.

TABLE V

CARBON FIBER STRAND PROPERTIES

Run No.	Short Gauge Tensile Strength Average GPa	Average (10^3 psi)	Maximum GPa	Maximum (10^3 psi)	Average Young's Modulus GPa	Average Young's Modulus (10^6 psi)	Avg. Break Strain (%)
11-7A	1.47	213	1.87	271	207	30	0.71
11-8	1.74	252	1.84	267	276	40	0.63
11-13	1.68	244	1.88	273	---	--	----
11-15A	1.63	236	1.99	287	262	37	0.62
11-16A	1.63	236	1.98	287	234	34	0.70

To test the capability of our line at this stage, pitch yarn was processed continuously through 1000°C with only one break in the yarn in four hours of operation to give 70 meters of carbonized material. This product exhibited an average strand tensile strength of 1.27 GPa (184 x 10^3 psi) and a Young's modulus 131 GPa (19 x 10^6 psi). After heating to 1650°C, the average strand tensile strength increased to 1.63 GPa (236 x 10^3 psi) and the modulus increased to 262 GPa (38 x 10^6 psi).

In the next stage of its development, the continuous pitch fiber line was expanded to include the final heat-treatment step at 1650°C, eliminating the need for winding and unwinding the yarn after carbonization at 1000°C. The 1650°C heat-treatment was carried out in a carbon tube furnace with an automatic control of temperature measured with a tungsten-rhenium alloy thermocouple.

2. SDO Experiment

The effect of processing parameters on fiber properties was studied in a series of experiments performed on the same yarn. A Self Directing Optimization scheme was employed because of the large number of interdependent variables. So far, twenty experiments were performed under varied conditions. The results in Table VI show that the carbonized fiber properties are indeed influenced by changes in processing conditions. Strand tensile strength varied between 0.83 GPa (121 x 10^3 psi) and 1.70 GPa (247 x 10^3 psi). Young's modulus ranged from 159 GPa (23 x 10^6 psi) to 214 GPa (31 x 10^3 psi). Individual single filaments with strengths of 2.00 GPa (300 x 10^3 psi) appeared in 70 percent of the samples. In general, the strand tensile strength was about 10 percent lower than the long gauge single filament values but the maximum strand test values sometimes approached the average short gauge values. On the other hand, the average Young's modulus from the strand test was mostly higher than the average modulus from the long gauge tests on single filaments. The SDO experiment is not yet completed at this writing, but significant improvements in fiber properties have been already achieved.

3. Sample Preparation

After achieving a smooth operation of the continuous line, several attempts were made to prepare larger amounts of yarn. In a successful experiment, five hours of continuous operation yielded 100 meters of yarn carbonized to 1650°C. The fiber contained 120 filaments with an average carbonized filament diameter of 13μm. Average fiber properties were: short gauge tensile strength, 1.95 GPa (283 x 10^3 psi); Young's modulus, 241 GPa (35 x 10^6 psi); strand tensile strength, 1.41 GPa (205 x 10^3 psi). This sample was sent to AFML.

TABLE VI

CARBON FIBER PROPERTIES OBTAINED IN THE COURSE OF THE SDO EXPERIMENT

SDO Exp.	Tensile Strength in GPa*					Young's Modulus in GPa*	
	Strand		Single Filaments				
	Avg.	Max.	Avg. Long Gauge	Avg. Short Gauge	Max. Short Gauge	Strand	Single Fil.
1	1.19	1.33	1.54	1.45	1.92	193	165
2	0.99	1.15	1.08	1.09	1.46	172	165
3	0.83	1.04	1.03	1.11	1.93	159	200
4	1.29	1.46	1.69	1.80	2.28	207	180
5	1.42	1.54	1.13	1.71	2.34	200	145
6	1.40	1.57	2.13	1.88	2.86	179	159
7	0.99	1.21	1.59	2.01	2.90	159	200
8	1.32	1.45	0.97	0.79	1.12	186	159
9	1.19	1.35	0.77	0.97	1.40	193	138
10	1.30	1.74	2.14	0.99	2.57	186	152
11	1.55	1.74	1.29	1.29	1.87	207	145
12	1.55	1.86	1.24	1.68	2.34	207	145
13	1.21	1.39	1.79	1.82	2.25	172	180
14	1.32	1.85	1.90	1.59	2.07	165	152
15	1.52	1.86	1.12	1.52	2.43	214	152
16	1.26	1.59	1.87	1.88	2.82	214	186
17	1.14	1.67	1.59	1.95	2.54	193	179
18	1.29	1.59	1.86	2.34	3.32	179	152
19	1.62	1.86	1.74	2.40	3.25	159	145
20	1.70	1.98	1.96	2.50	3.01	166	165

*Multiply by 1.45×10^5 to convert to psi units.

Since the standard processing rate was only 20 meters per hour, the accumulation of large amounts of 120 filament yarn was tedious, particularly in quantities needed for the preparation and evaluation of composites. To increase the volume of material, 480 filament pitch yarn was made by plying together four 120 filament strands. The processing of the four-ply yarn was carried out with conditions identical to those used for 120 filament strands. Properties of the final (1650°C) product were lower than desired.

The processing of 240 filament yarn proved to be more successful; approximately 400 meters of carbonized (1650°C) fiber were produced at speeds of 25 to 35 meters per hour. The yarn had an average strand tensile strength of 1.77 GPa (256 x 10^3 psi) and a Young's modulus of 228 GPa (33 x 10^6 psi). The complete test results are given in Table VII. The highest average strand tensile strength (1.89 GPa, 274 x 10^3 psi) was obtained at the slowest processing speed. The corresponding single filament properties were: long gauge tensile strength, 2.24 GPa (326 x 10^3 psi); short gauge tensile strength, 2.19 GPa (317 x 10^3 psi); Young's modulus, 283 GPa (41 x 10^6 psi).

TABLE VII

STRAND TEST DATA FOR 240 FILAMENT YARN HEAT-TREATED TO 1650°C

Sample 571-11-53A		Sample 571-11-53B		Sample 571-11-53C	
Tensile St., GPa	Young's Modulus, GPa	Tensile St., GPa	Young's Modulus, GPa	Tensile St., GPa	Young's Modulus, GPa
1.45	213	1.99	207	1.50	221
1.44	213	2.03	228	1.84	234
1.80	---	2.11	---	1.78	---
1.74	---	1.76	---	1.45	---
2.05	---	1.88	---	1.93	---
1.83	---	1.26	---	1.97	---
1.69	---	1.99	---	1.72	---
1.76	---	1.90	---	1.68	---
1.74	---	2.03	---	1.83	---
2.12	---	1.93	---	1.92	---
avg. 1.76	213	avg. 1.89	218	avg. 1.74	228
(256 x 10^3 psi)	(31 x 10^6 psi)	(275 x 10^3 psi)	(32 x 10^6 psi)	(252 x 10^3 psi)	(33 x 10^6 psi)
density = 2.10 Mg/m^3		density = 1.99 Mg/m^3		density = 2.00 Mg/m^3	

Multiply by 1.45 x 10^5 to convert to values in psi.

SECTION VI

PROCESSING AND PROPERTIES OF ULTRAFINE FILAMENTS

During the previous contract period, maximum strengths approaching 3.50 GPa (500 x 10^3 psi) were obtained on some filaments with as-spun diameters of 10μm or less. These findings prompted a systematic effort to raise the average properties to these levels. Ten series of experiments were done with different batches of ultrafine filaments with average diameters between 7.7μm and 9.6μm. In each series the procedure consisted of varying the thermosetting conditions, while keeping the carbonizing conditions constant. The final heat-treatments were usually 1500°, 1650°, and 1800°C. The processed filaments were evaluated by single filament tests both at 20 mm and 3 mm gauge length.

Previous experience indicated that the properties of carbon fibers from MP pitches are largely determined in the thermosetting stage. Therefore, a broad range of thermosetting conditions was explored in each experimental series. Surprisingly, no consistent effect of thermosetting on the filament properties was apparent in these experiments. Either the thermosetting times used were not critical in these thin filaments or variations in filament diameter and filament quality were more important in determining the level of final properties. Increasing the final heat-treatment temperature generally raises the elastic modulus, but again this effect was not consistently present in these experiments. Some of the best results, obtained at a final heat-treatment of 1650°C, are shown in Table VIII. Both the filament strength and the elongation-to-break achieved in most samples are very promising. The tensile strengths, 3.56 GPa (520 x 10^3 psi) long gauge and 4.14 GPa (600 x 10^3 psi) short gauge, measured on sample C are the highest average values ever observed on pitch carbon fibers. Tables IX and X reproduce the computer printouts of the single filament tests for this sample.

The average mechanical properties from all ten experimental series are: short gauge tensile strength, 3.10 GPa (450 x 10^3 psi); modulus, 276 GPa (40 x 10^6 psi); elongation-to-break, 1.1 percent. At least 4 breaks on individual filaments gave strengths close to 7.0 GPa (1 x 10^6 psi), indicating that even the best average properties achieved still fall short of the ultimate potential of our fibers.

Final heat-treatment to 1550°C generally results in lower properties as shown in Table XI. The comparison of individual samples with those in Table VIII illustrates the previously mentioned lack of systematic correlation between the final heat-treatment temperature and the properties. The last entry in Table XI shows a particularly attractive combination of 290 GPa (42 x 10^6 psi) for the elastic modulus with 3.59 GPa (520 x 10^3 psi) for the long gauge tensile strength.

TABLE VIII

AVERAGE PROPERTIES OF ULTRAFINE FILAMENTS
HEAT-TREATED AT 1650°C

Sample	No. Fil. Tested	Fil. Diam. μm	Tensile Strength GPa	Tensile Strength (10^3 psi)	Young's Modulus GPa	Young's Modulus (10^6 psi)	El. to Break %
A-L	3	7.2	1.59	230	144	21	1.2
A-S	5	7.4	1.65	240			
B-L	14	4.8	3.52	510	413	60	0.8
B-S	6	4.9	3.45	500			
C-L	10	4.8	3.45	510	441	64	0.9
C-S	8	4.8	4.14	600			
D-L	4	5.7	2.41	350	290	42	1.1
D-S	5	5.3	3.17	460			
E-L	4	5.8	2.28	330	303	44	0.8
E-S	4	5.8	2.34	340			
F-L	11	5.2	3.12	450	400	58	0.7
F-S	12	5.6	2.76	400			
G-L	2	5.4	3.03	440	255	37	1.6
G-S	6	5.4	4.00	580			
H-L	6	5.7	2.69	390	248	36	1.4
H-S	6	6.0	3.45	500			
I-L	2	5.3	1.93	280	200	29	1.9
I-S	7	6.7	3.72	540			
J-L	6	5.5	1.59	230	255	37	1.3
J-S	5	5.8	3.45	500			

L - long gauge test.

S - short gauge test.

TABLE IX

LONG GAUGE PROPERTIES OF INDIVIDUAL FILAMENTS FROM SAMPLE 571-11-21B

DATE 8-2-73

SUBMITTED BY DIDCHENKO
CHARGE NUMBER 817-2413
SAMPLE 13071607-3
COMPLIANCE ADJUSTMENT 0.080
MAGNIFICATION/MICROSCOPE CORRECTION FACTOR 0.1818

LENGTH (CM.)	BREAKING FORCE(GM.)	COMPLIANCE (.001 CM./GM.)	C/L (.001/GM.)	TENS. STRENGTH (LBS./SQ. IN.)	YOUNGS MOD. (LBS./SQ. IN.)	AREA (SQ. MICRONS)
0.198E 01	0.536E 01	0.220E 01	0.115E 01	0.665E 06	0.107E 09	0.11447E 02
0.198E 01	0.583E 01	0.204E 01	0.103E 01	0.603E 06	0.100E 09	0.13732E 02
0.198E 01	0.553E 01	0.383E 01	0.193E 01	0.415E 06	0.387E 08	0.18923E 02
0.198E 01	0.743E 01	0.255E 01	0.129E 01	0.423E 06	0.441E 08	0.24946E 02
0.198E 01	0.595E 01	0.260E 01	0.131E 01	0.415E 06	0.530E 08	0.20351E 02
0.198E 01	0.575E 01	0.237E 01	0.120E 01	0.327E 06	0.474E 08	0.24946E 02
0.198E 01	0.699E 01	0.287E 01	0.145E 01	0.566E 06	0.557E 08	0.17547E 02
0.198E 01	0.732E 01	0.259E 01	0.131E 01	0.641E 06	0.669E 08	0.16224E 02
0.198E 01	0.555E 01	0.332E 01	0.167E 01	0.527E 06	0.566E 08	0.14952E 02
0.198E 01	0.695E 01	0.276E 01	0.139E 01	0.660E 06	0.680E 08	0.14952E 02
0.197E 01	0.626E 01	0.272E 01	0.137E 01	0.524E 06	0.638E 08	0.17802E 02

0.45408E 01 STD. DEV. AREA OR 25.5 PERCENT

0.251E-06 STD. DEV. LENGTH OR 0.0 PER CENT
0.808E 00 STD. DEV. BREAKING FORCE OR 12.9 PER CENT
0.521E 00 STD. DEV. COMPLIANCE OR 19.1 PER CENT
0.263E 00 STD. DEV. COMPLIANCE/LENGTH OR 19.1 PER CENT

0.665E 06 MAX. TENSILE STRENGTH (LBS./SQ. IN.)
0.327E 06 MIN. TENSILE STRENGTH (LBS./SQ. IN.)
0.121E 06 STD. DEV. TENSILE STRENGTH OR 23.1 PER CENT

0.107E 09 MAX. YOUNGS MODULUS (LBS./SQ. IN.),
0.387E 08 MIN. YOUNGS MODULUS (LBS./SQ. IN.),
0.230E 08 STD. DEV. YOUNGS MODULUS, OR 36.0 PER CENT

TABLE X

SHORT GAUGE PROPERTIES OF INDIVIDUAL FILAMENTS FROM SAMPLE 571-11-21B

DATE 8-2-73

SUBMITTED BY DIDCHENKO
CHARGE NUMBER 817-2314
SAMPLE 13071607-4
COMPLIANCE ADJUSTMENT 0.000
MAGNIFICATION/MICROSCOPE CORRECTION FACTOR 0.1818

LENGTH (CM.)	BREAKING FORCE (GM.)	COMPLIANCE (.001 CM./GM.)	C/L (.001/GM.)	TENS. STRENGTH (LBS./SQ. IN.)	YOUNGS MOD. (LBS./SQ. IN.)	AREA (SQ. MICRONS)
0.320E 00	0.654E 01	0.000E 00	0.000E 00	0.398E 06	0.000E 00	0.23308E 02
0.320E 00	0.528E 01	0.000E 00	0.000E 00	0.462E 06	0.000E 00	0.16224E 02
0.320E 00	0.803E 01	0.000E 00	0.000E 00	0.997E 06	0.000E 00	0.11647E 02
0.320E 00	0.838E 01	0.000E 00	0.000E 00	0.867E 06	0.000E 00	0.13732E 02
0.320E 00	0.787E 01	0.000E 00	0.000E 00	0.512E 06	0.000E 00	0.21831E 02
0.320E 00	0.503E 01	0.000E 00	0.000E 00	0.286E 06	0.000E 00	0.24946E 02
0.320E 00	0.763E 01	0.000E 00	0.000E 00	0.725E 06	0.000E 00	0.14958E 02
0.320E 00	0.305E 01	0.000E 00	0.000E 00	0.229E 06*	0.000E 00	0.18923E 02
0.319E 00	0.647E 01	0.000E 00	0.000E 00	0.560E 06 0.607E 06	0.000E 00	0.18177E 02

0.40679E 01 STD. DEV. AREA OR 26.7 PERCENT

0.127E-06 STD. DEV. LENGTH OR 0.0 PER CENT
0.187E 01 STD. DEV. BREAKING FORCE OR 28.9 PER CENT
0.000E 00 STD. DEV. COMPLIANCE OR 0.0 PER CENT
0.000E 00 STD. DEV. COMPLIANCE/LENGTH OR 0.0 PER CENT

0.997E 06 MAX. TENSILE STRENGTH (LBS./SQ. IN.)
0.229E 06 MIN. TENSILE STRENGTH (LBS./SQ. IN.)
0.276E 06 STD. DEV. TENSILE STRENGTH OR 49.3 PER CENT

0.000E 00 MAX. YOUNGS MODULUS (LBS./SQ. IN.).
0.000E 00 MIN. YOUNGS MODULUS (LBS./SQ. IN.).
0.000E 00 STD. DEV. YOUNGS MODULUS. OR 0.0 PER CENT

*This value is outside the limits of the standard deviation. The average tensile strength of the seven remaining filaments is 607 x 10^3 psi.

TABLE XI

PROPERTIES OF ULTRAFINE MONOFILAMENTS
PROCESSED TO 1550°C

Sample	No. Fils. Tested	Diam. μm	Tensile Strength GPa	(10^3 psi)	Young's Modulus GPa	(10^6 psi)	El. to Break %
12-96a	7	6.5	2.34	340	174	25	---
	6*	7.3	2.55	370	---	--	1.5
12-96b	7	5.8	2.28	330	207	30	---
	6*	6.8	2.34	340	---	--	1.1
12-96c	6	5.7	1.65	240	268	39	---
	5*	6.3	2.34	340	---	--	0.9
14-13a	7	5.5	2.96	430	268	39	---
	7*	6.8	3.18	460	---	--	1.2
14-13b	7	4.9	2.55	370	324	47	---
	6*	7.1	2.28	330	---	--	0.7
14-13c	7	6.3	3.58	520	290	42	---
	7*	6.9	3.30	480	---	--	1.2

*Short gauge tensile test.

The diameters of the carbonized filaments ranged from 5.7 to 7.1μm; reflecting a 50 percent reduction in the cross-sectional area of the raw pitch fibers. Simultaneously, the fiber density increases from about 1.35 Mg/m^3 in the as-spun state to about 2.1 Mg/m^3 in the processed filaments. The filaments shrunk 11 to 12 percent in length during processing up to 1000°C. No measurable effects occurred above that temperature.

SECTION VII

THERMOSETTING WITH NITROGEN DIOXIDE

The thermosetting of pitch fibers in oxygen or air is relatively slow. The process is significantly faster when the fiber is pretreated in a liquid oxidizing bath, but there are some inherent disadvantages associated with the treatment. Therefore, search for rapid gaseous thermosetting agents has been continued.

In the patent literature,[4] there are several references to nitrogen dioxide as a very effective thermosetting agent for pitch fibers. It was of interest to establish whether this reagent has any advantages for use with MP pitch fibers. Nitrogen dioxide is indeed unique as a thermosetting agent for MP pitch fibers in that the gas is effective at room temperature with the usual second stage heat-treatment in oxygen being optional. Exposure to nitrogen dioxide for periods as brief as 15 to 30 seconds renders the pitch fibers infusible. Table XII shows the results of a study of the fiber properties as a function of thermosetting severity in nitrogen dioxide. Yarn with about 15μm filament diameter was used. After carbonization, the filaments had diameters of about 10μm. It is apparent that the additional oxygen treatment had no pronounced effect on fiber properties. The strength levels tend to increase with the degree of thermosetting and are comparable to those achieved by our standard thermosetting; the elastic moduli tend to be relatively high.

A second group of experiments brought to light some difficulties associated with this manner of thermosetting. After more intensive treatment with nitrogen dioxide, some samples reacted violently with oxygen causing destruction of the fiber. In these tests, pitch fibers were exposed from 120 to 300 seconds to nitrogen dioxide at room temperature, and, in some cases, infusibilization was continued by heating the fibers in oxygen. Several of the nitrogen dioxide treated pitch samples ignited in the hot oxygen. The experimental conditions and the results are shown in Table XIII. The surviving fibers again follow the trend of increasing tensile strengths with the exposure to nitrogen dioxide. Surprisingly, the properties achieved with thinner fibers (B) were not better than those of the thicker fibers (A).

The chemical analysis revealed that pitch fibers treated for 30 seconds in nitrogen dioxide had O, 11.8 percent; N, 1.84 percent; O/N atomic ratio, 5.6. Much longer, 30 minutes, exposure to nitrogen dioxide produced a fiber with the composition: O, 34.2 percent; N, 2.67 percent; O/N atomic ratio, 11.2. It is apparent that both oxidation and nitration are occurring simultaneously, with oxidation being dominant during the longer exposure. The mechanism of the nitrogen-dioxide-pitch reaction is not known but a variety of products can be expected. Aromatic compounds generally react with NO_2 to give substituted nitro products; however, quinones and carboxyl groups also may form.

TABLE XII

SINGLE FILAMENT PROPERTIES OF CARBONIZED FIBERS (1650°C)
PREPARED WITH NITROGEN DIOXIDE THERMOSETTING

Sample	Time in NO_2, sec.	Oxygen Treatment	Tensile Strength						Young's Modulus	
			Avg. Long Gauge GPa	Avg. Long Gauge (10^3 psi)	Avg. Short Gauge GPa	Avg. Short Gauge (10^3 psi)	Max. Short Gauge GPa	Max. Short Gauge (10^3 psi)	GPa	(10^6 psi)
1A-2	15	yes	1.35	196	1.50	217	2.07	301	303	44
1B-1	30	no	1.24	180	1.48	214	2.16	313	351	51
1B-2	30	yes	1.50	218	1.46	211	2.12	308	321	48
1C-2	60	yes	1.30	188	1.80	261	3.31	480	241	35
1D-1	90	no	1.17	170	1.74	252	3.01	436	283	41
1D-2	90	yes	1.85	269	1.22	177	1.54	223	321	48
1E-2	120	yes	1.30	189	1.25	181	1.86	270	290	42
1F-1	180	no	1.63	236	2.10	305	5.11	741	359	52
1F-2	180	yes	2.21	321	2.61	379	7.86	1140	517	75

TABLE XIII

SINGLE FILAMENT PROPERTIES OF CARBONIZED FIBERS (1650°C)
PREPARED WITH NITROGEN DIOXIDE THERMOSETTING

Fiber Batch	Time in NO_2, sec.	Oxygen Treatment	Tensile Strength Avg. Short Gauge GPa	Tensile Strength Avg. Short Gauge (10^3 psi)	Tensile Strength Max. Short Gauge GPa	Tensile Strength Max. Short Gauge (10^3 psi)	Young's Modulus GPa	Young's Modulus (10^6 psi)	Carbonized Filament Diameter, μm
A	120	no	1.29	187	2.09	303	248	36	10
A	180	no	1.35	196	1.81	263	345	50	"
A	180	no	1.35	195	1.94	281	207	30	"
A	390	no	2.54	339	3.51	518	317	46	"
A	180	yes	Burned in O_2						"
A	300	yes	Burned in O_2						"
B	120	no	1.35	196	1.65	239	221	32	6
B	120	yes	1.55	225	1.67	242	152	22	"
B	180	yes	Burned in O_2						"
B	240	no	1.83	266	2.76	400	131	19	"
B	240	yes	2.42	351	2.68	389	276	40	"

The extremely corrosive and noxious nature of nitrogen dioxide makes the experimentation with this gas very difficult. Furthermore, the possibility of inadvertently producing something akin to TNT discouraged us from continuing this study inspite of the rather promising properties.

SECTION VIII

FIBER STRUCTURE

The mechanical properties of carbon fibers depend upon their structure. It is, therefore, important to correlate the structure and the properties as a guide for improving properties and optimizing processing variables. The structural techniques which have been found most useful are X-ray diffraction, polarized light microscopy (PLM), and scanning electron microscopy (SEM). Some preliminary efforts have also been made to utilize transmission electron microscopy (TEM).

In the next section, these techniques are described and the type of information that can be derived from them is discussed. As the quality and uniformity of our fibers improved and their diameters decreased, certain structural features seemed to change while others did not. It is, therefore, instructive to compare the early observations on larger diameter, nonuniform fibers with those obtained more recently. The experimental results for several examples of fibers made at different times under different spinning and processing conditions are presented and discussed in Section 2.

1. Experimental Techniques

a. X-ray Diffraction

The degree of preferred orientation of carbon layer planes along the fiber axis and the apparent crystalline stack height (L_c) were obtained from flat-plate diffraction patterns. Bundles of single filaments or several strands of multifilament yarn were inserted into thin-walled (10μm) glass capillary tubes of 0.7 mm I.D. Each sample was then cut to ~20 mm length and positioned vertically in front of the X-ray beam. The flat-plate film holder was placed 30 mm from the sample. For this geometry, exposures of 0.5 to 2 hours with 45 Kv copper (K_α) X-ray radiation were required to obtain adequate contrast on the film.

The films were analyzed on a Joyce-Loebl microdensitometer by taking a series of radial scans at 3° (2θ) intervals. The degree of preferred orientation, FWHM (full-width at half-maximum of the azimuthal intensity distribution), was obtained from the microdensitometer tracings of the (002) arcs as described previously.[5] The crystalline stack height (L_c) was determined by means of the reduced Scherrer equation $L_c = \frac{90}{\Delta(2\theta)}$ where $\Delta(2\theta)$ is the width of the central peak.

Since these MP carbon fibers are graphitizable, accurate d-spacings were obtained with a standard cylindrical camera from the (00ℓ) lines of 3000°C heat-treated fibers. The three-dimensional order diffraction lines were used as an indication of the degree of graphitic character.

b. Polarized Light Microscopy (PLM)

The size, uniformity, and relative orientation of the anisotropic domains in the fibers were obtained from PLM observations. The fibers were encapsulated in an epoxy resin so that either transverse or longitudinal sections could be examined. The samples were first ground on silicon carbide laps, then polished successively on diamond paste laps and finally on a microcloth saturated with a 0.3 percent suspension of alumina in water. The polished samples were examined with a Bausch & Lomb metallograph under crossed polarizers at magnifications up to 1000X.

Although the optical anisotropy of fibers is readily observed under crossed polarizers, there still remains some ambiguity concerning the actual orientation of layers in the fibers. For example, since layer orientations either parallel or perpendicular to the crossed polarizer directions exhibit extinction, certain obviously different fiber structures, such as a radial or an onionskin structure, would not be distinguishable.

However, the insertion of a sensitive tint plate would permit the two types of structures to be distinguished.[6] Figure 7 illustrates schematically the comparison of the two types of fiber structures with higher-oriented pyrolytic graphite as an orientation standard. It should be emphasized that the actual shades and intensities of colors depend critically on the particular microscope setup, type and thickness of the sensitive tint plate, optical filters, camera, exposure, and type of photographic film used to record the observations. However, if all observations are made on the same microscope under identical conditions for both the fibers and the pyrolytic graphite standard, no ambiguities arise. For the particular Bausch & Lomb microscope employed, the observed color scheme was, B - blue, P - pink, and M - magenta. The layer orientations corresponding to these colors are shown in (a) for the pyrolytic graphite standard. The color patterns for the two types of fiber structure are illustrated schematically in (b) and (c). The maltese crosses in both structures were magenta, since as indicated in (a), the parallel and perpendicular orientations are indistinguishable. However, the blue and pink colors in (b) and (c) were precisely reversed. The only structures consistent with the observed color schemes would be the radial (b) and the onionskin (c).

c. Scanning Electron Microscopy (SEM)

Scanning electron microscopy of fractured fibers gives an indication of the type of flaws in the fibers and also yields information about the microstructure of the fibers. Flaws of defects are revealed because the fiber will often break at the flaw. Microstructural information can often be inferred from the fracture surfaces because of the high magnification, up to 10,000X, and the appreciable depth of focus of the SEM.

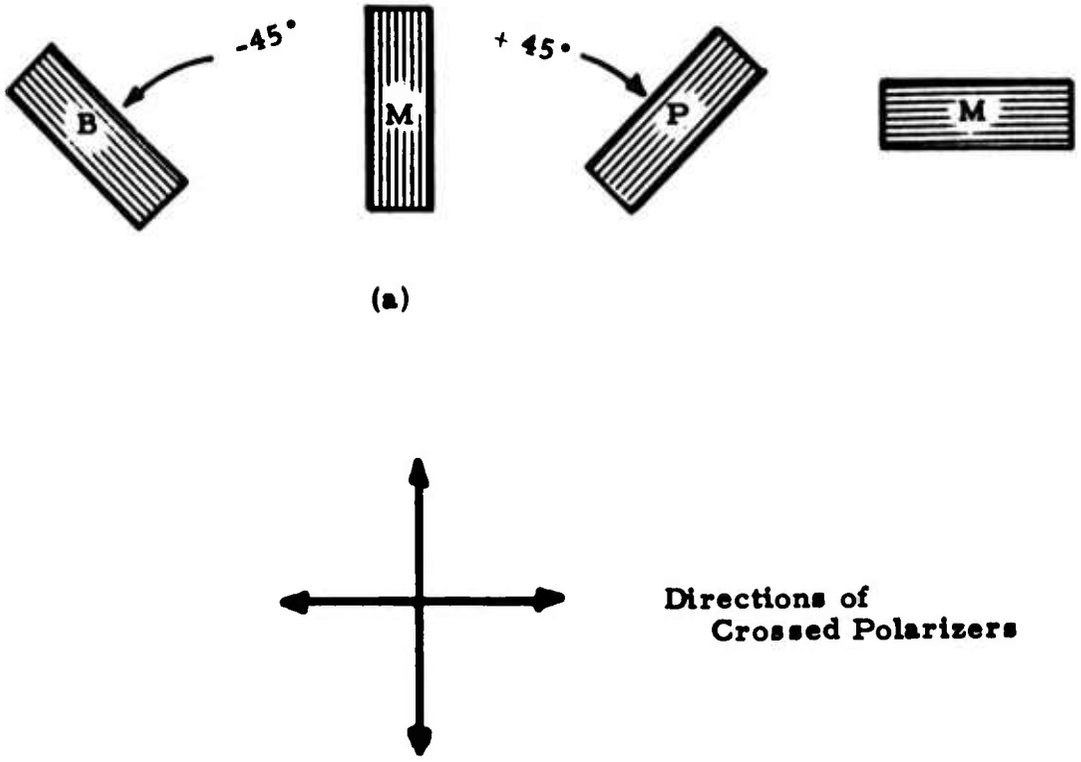

Figure 7. Schematic Diagram of Sensitive Tint Observations
(a) Edge Views of Highly Oriented Pyrolytic Graphite,
(b) Cross-Section of Fiber with Radial Structure,
(c) Cross Section of Fiber with an Onionskin Structure.
The Colors are Represented by, B - Blue, P - Pink,
and M - Magenta

Samples for examination by SEM were prepared by manually fracturing a bundle of filaments in tension, mounting the fractured fibers in a holder, and coating the fibers with a gold film. The "MAC 700" Scanning Electron Microscope was used.

d. Transmission Electron Microscopy (TEM)

Transmission electron microscopy enables one to study the finest microstructural details of carbon fibers at greater magnifications than those obtainable by SEM. In addition, the application of selected area electron diffraction techniques can provide information on the layer orientation both along and across the fiber. However, sample preparation for TEM is much more difficult and tedious than for SEM, and the initial effort was limited to the evaluation of several sample preparation techniques and modes of observation.

2. Results and Discussion

a. Early Batch-Processed Fibers

These fibers, 10-20μm in diameter, were thermoset at several different levels of severity and subsequently heated to 1500° or 3000°C. X-ray diffraction, PLM, and SEM measurements were made on this series of samples.

(1) X-ray Diffraction

The degree of preferred orientation (FWHM) and crystalline stack height (L_c) were similar to the values determined previously on thicker fibers, namely, about 30° and 3nm, respectively.[7] The degree of preferred orientation for all the 1500°C heat-treated samples was approximately the same and seemed to be independent of the thermosetting level. The crystalline stack height of about 2.2nm indicates some degradation in crystallinity compared to the as-spun and thermoset fibers, but the crystalline perfection and degree of preferred orientation increased rapidly with heat-treatment temperature above 1500°C. The patterns for single filaments of 3000°C heat-treated fibers were extremely sharp, the FWHM being between 5° and 10°, and L_c greater than 10nm. The interlayer spacings of the 3000°C fibers (average of 004 and 006 lines) were 0.3367 ± 0.0003nm and independent of the degree of thermosetting. On the other hand, the degree of three-dimensional order, as manifested by the resolution of the (10) band and the diffuseness of the (112) line, indicated a slight decrease in three-dimensional order with increasing degree of thermosetting.

(2) Microscopy Examinations

Polarized light micrographs of the as-spun and thermoset fibers were similar; some severely thermoset fibers are shown in Figure 8.

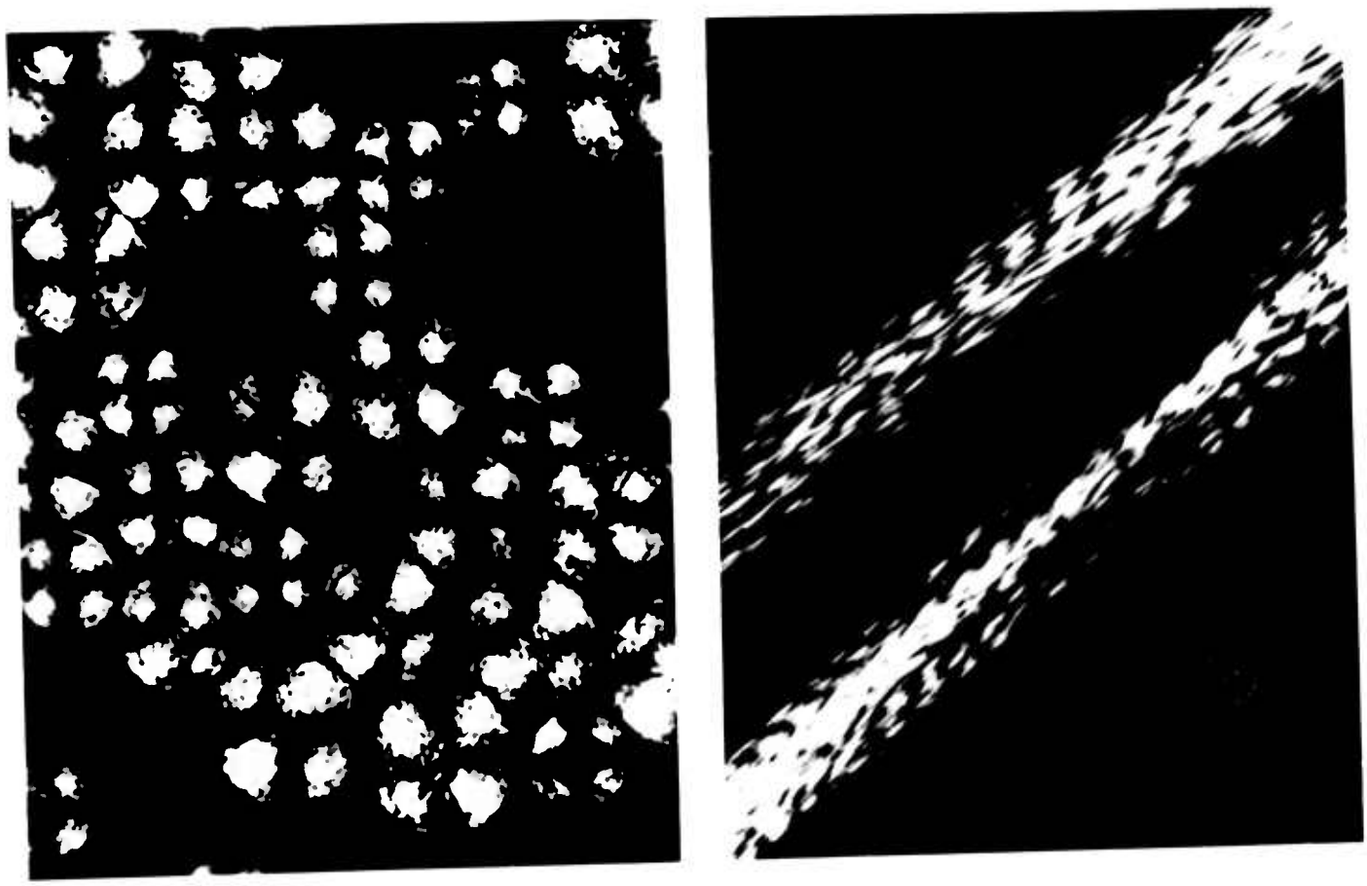

(a) (b)

20μm

Figure 8. Polarized Light Photomicrographs of Severely Thermoset MP Fibers (1000X)

(a) Cross Section
(b) Longitudinal Section

The distinct, symmetrical maltese cross patterns in the cross sections (Fig. 8a) indicate cylindrical symmetry of the layer orientation. Under sensitive tint, the configuration is found to be clearly radial and not onionskin. There is essentially no change in this basic layer configuration up to 3000°C heat-treatment. The longitudinal section in Figure 8b indicates a small (1-3μm) and uniform domain size, however, the precise orientation of the sectioning plane can affect the appearance of the domains. The longitudinal sections of the 1500° and 3000°C heat-treated fibers were similar, but the domain size in the underthermoset fibers was clearly larger than in the overthermoset fibers.

SEM pictures of fractured thermoset fibers also showed some differences between the over and underthermoset fibers. The mildly thermoset fibers in Figure 9a show a featureless fracture surface, similar to that observed for as-spun fibers. On the other hand, the more extensively thermoset fiber in Figure 9b clearly shows the radial structure.

Figure 10 shows SEM pictures of 1500°C heat-treated fibers, with two different degrees of thermosetting. In (a), fibers show the radial structure, but there is considerable fiber fusion due to incomplete and nonuniform thermosetting. Also, the longitudinal cracks have become larger. In (b), the fibers again clearly show the radial structure but much less fusion has occurred between filaments, as these fibers have been thermoset more extensively.

Figure 11 shows pictures of 3000°C graphitized fibers which had been insufficiently thermoset. Some of the fibers are fused together and have the delaminated layer structure of incompletely thermoset, well-graphitized materials. Within the same group, other fibers appear to have had a glassy-type fracture. The lower picture (b) shows the layered structure at higher magnification.

In conclusion, although the fibers chosen for these early structural studies were of poor uniformity, the variety of both the X-ray and microscopy observations indicates that these methods are quite sensitive to fiber structure and processing parameters.

b. Observation of Onionskin Structures

In the previous section results were presented for a series of 10-20μm diameter fibers batch processed under various thermosetting and carbonizing conditions. A predominantly radial structure was inferred from both PLM and SEM. In some recently prepared ultrafine filaments (~5μm in diameter) a different structure has been observed, namely one more closely approximating a tree-trunk or onionskin structure. These structural differences were first observed by SEM, and then further confirmed by PLM with the sensitive tint techniques described in Section 1c.

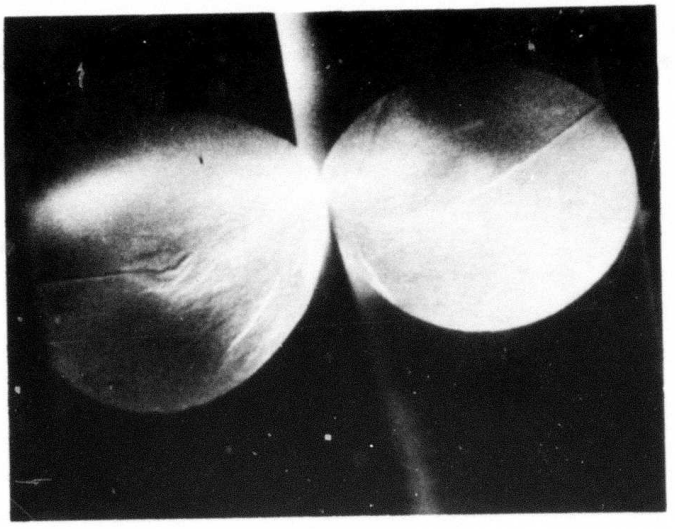

(a)

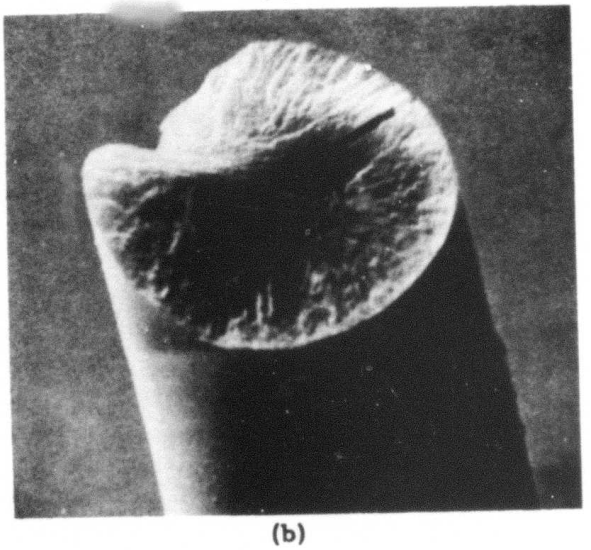

(b)

10μm

Figure 9. SEM Pictures of Fracture Surfaces of Thermoset Fibers

(a) Mild Thermosetting
(b) Severe Thermosetting

(a)

20μm

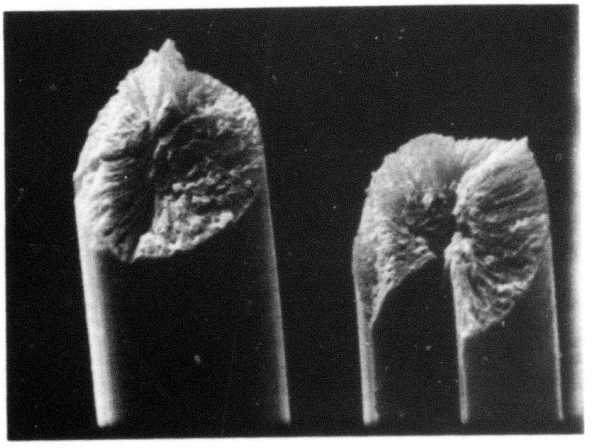

(b)

10μm

Figure 10. SEM Pictures of Fracture Surfaces of 1500°C Heat-Treated Fibers

(a) Mild Thermosetting
(b) Severe Thermosetting

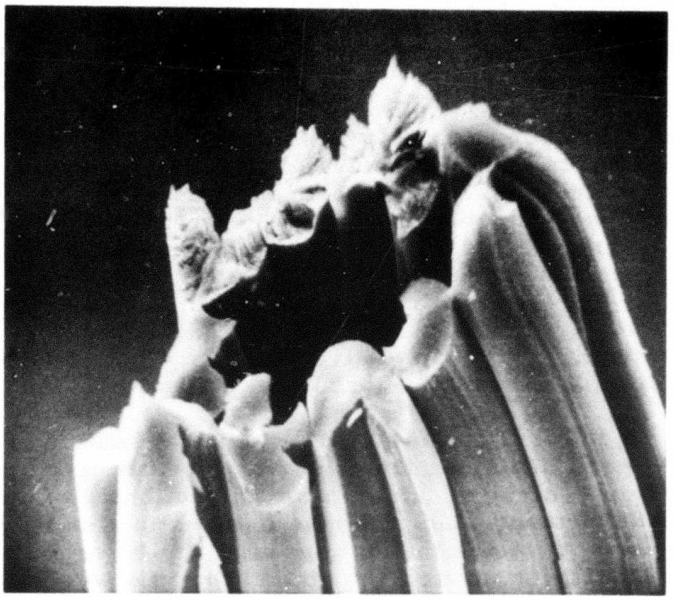

(a)

20μm

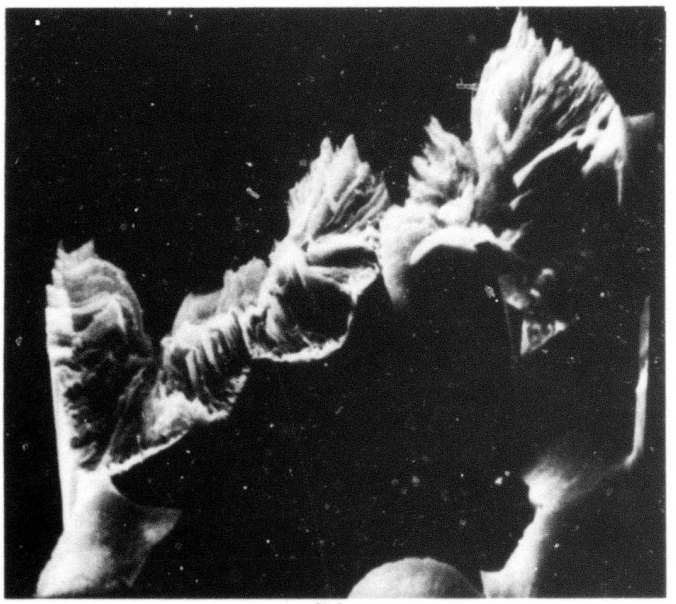

(b)

10μm

Figure 11. SEM Pictures of 3000°C Heat-Treated Underthermoset Fibers at Two Magnifications

Figure 12 shows an SEM comparison of the two types of structures, (a) the radial structure of a 10μm diameter fiber and (b) the onionskin structure of one of the 5μm diameter fibers. The fibers in (a) and (b) had been heat-treated at 1500°C and 1650°C, respectively. These structural differences were also detected in the as-spun fibers. Figure 13 compares PLM pictures of the two types of as-spun fiber, (a) those with radial structure and (b) those with onionskin structure. The structural differences are not apparent without the sensitive tint plate in PLM, since both Figures 13(a) and 13(b) indicate similar maltese cross extinction patterns which remain stationary with stage rotation. This invariance under rotation is to be expected since both radial and onionskin structures possess cylindrical symmetry. However, with the sensitive tint plate inserted, the color patterns of the two fibers were reversed in the manner indicated in Figure 7. It is also of interest that fiber diameter alone does not determine the type of structure, since considerably larger fibers (up to 10μm as-spun diameter) have been observed with an onionskin structure.

Figure 14 shows two views of a longitudinal section of one of the onionskin fibers. The dark line along the center of the fiber in (a) is consistent with an onionskin structure because, at any level of sectioning parallel to the central axis, such a structure would give rise to an extinction line or band as a result of looking directly along the optic axes of flat layer planes. In (b) the microscope stage had been rotated 45° so that the axis was parallel to one of the polarizer directions; extinction is seen to be almost complete. It should be emphasized that most monofilaments do not have a perfectly developed onionskin structure. Ordinarily, the structure is more random as seen in Figure 15, in which no maltese cross is observed.

c. Microscopy of Uniformly Processed Fibers

As fibers with improved uniformity became available, attempts to correlate fiber processing and structure with fiber properties were resumed. The first effort was a PLM and SEM study of the effect of two very different thermosetting conditions on the structure and properties of carbonized fibers. A cross section of the raw multifilament yarn used for this study is shown in Figure 16. The filaments exhibit a radial layer plane orientation and most have a radial crack. Several samples from this batch were processed under varying conditions. The micrographs of the carbonized fibers with the better properties are shown in Figure 17. This sample had a tensile strength of 1.55 GPa (225×10^3 psi) and a Young's modulus of 207 GPa (30×10^6 psi) determined by the strand test. Evidently, the split in the as-spun fiber spread into a wedge during processing. The fine-grained appearance in the cross section has been preserved during the thermosetting.

(a)

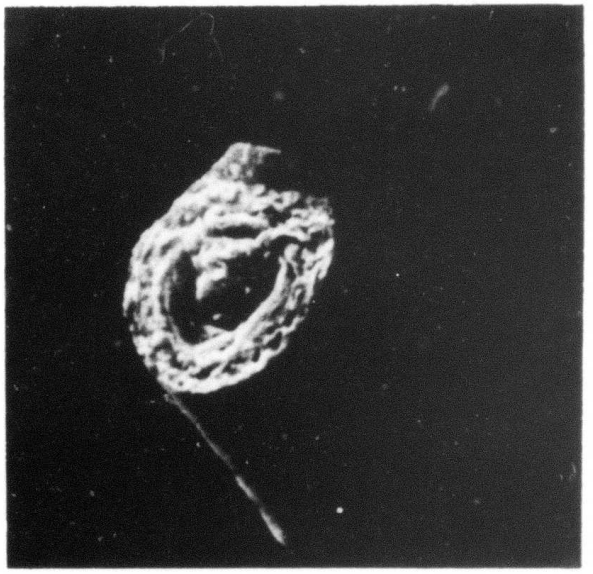

(b)

Figure 12. SEM Pictures of Fracture Surfaces of the Two Types of Fibers

(a) Radial Structure of a 10μm Fiber Carbonized at 1500°C
(b) Onionskin Structure of a 5μm Fiber Carbonized at 1650°C

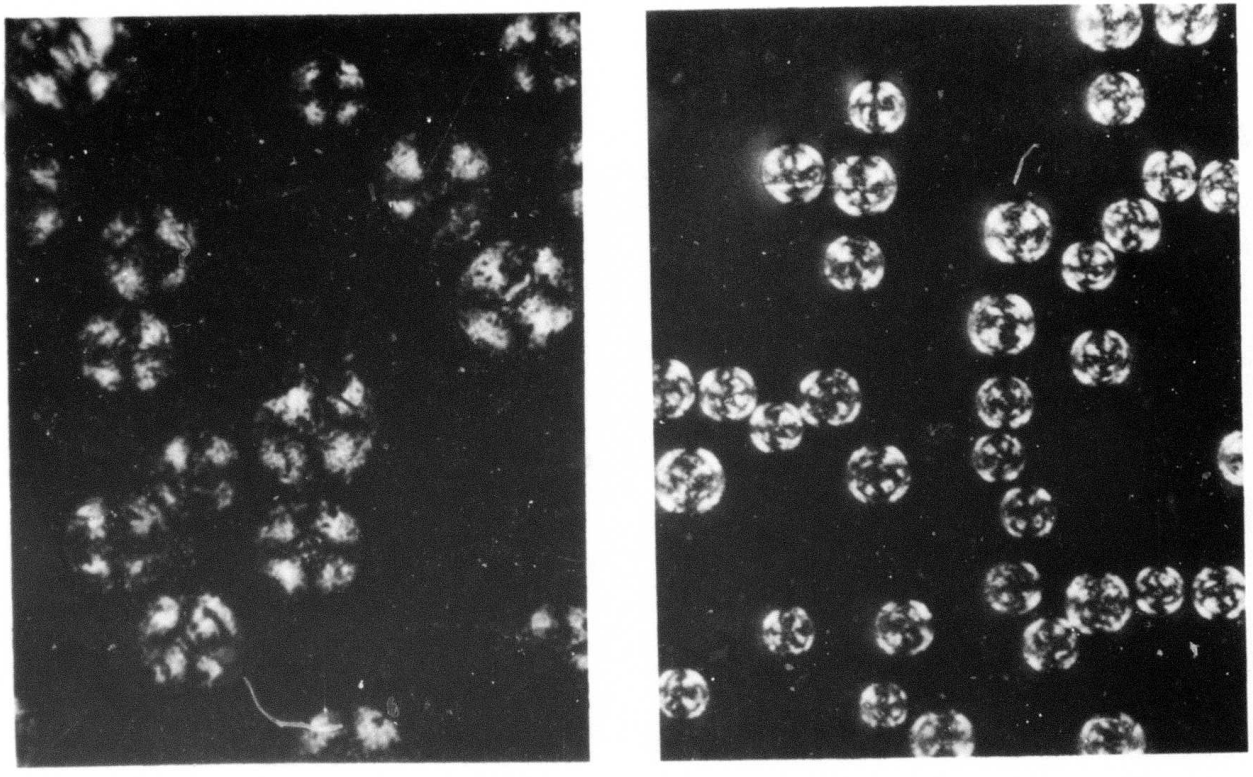

Figure 13. PLM Pictures of As-Spun Fibers of the Two Structural Types.

(a) Radial
(b) Onionskin

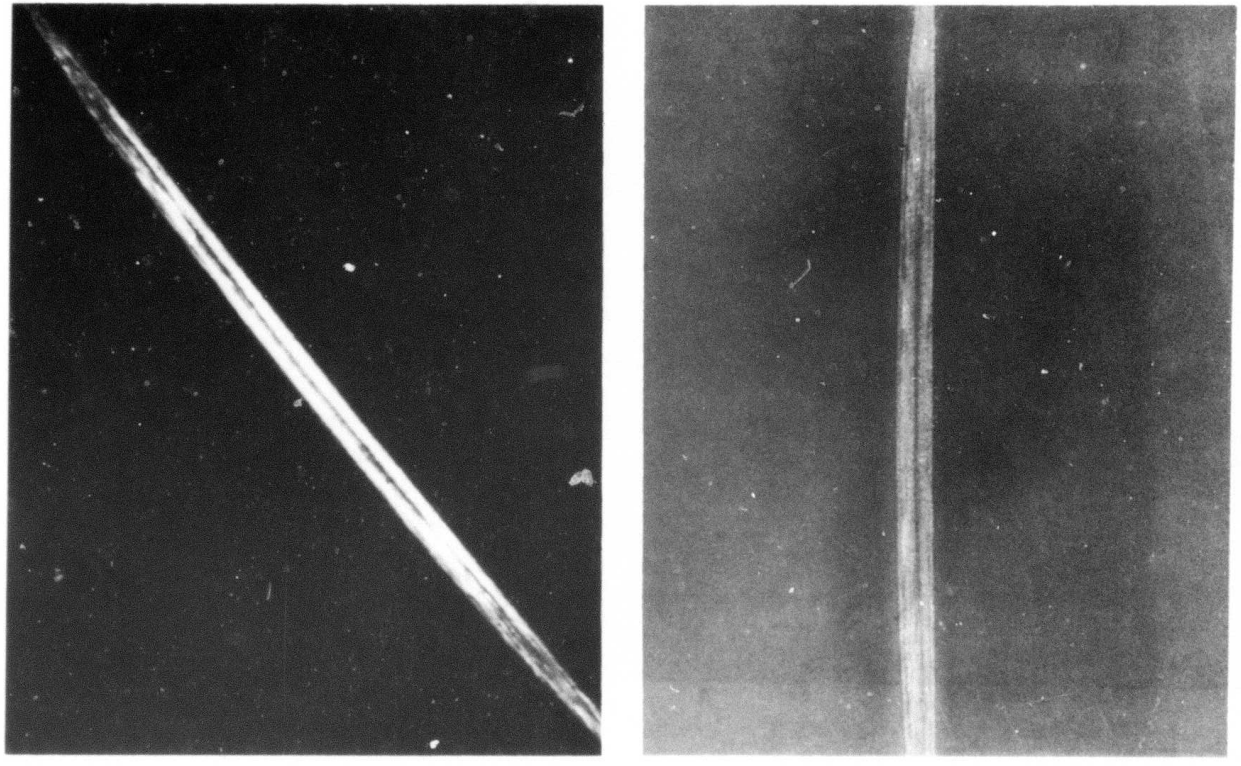

(a) (b)

Figure 14. PLM Pictures of Longitudinal Section of a Fiber with Onionskin Structure

In (a) fiber axis is at 45° to polarizer directions.
In (b) fiber axis is parallel to one polarizer direction.

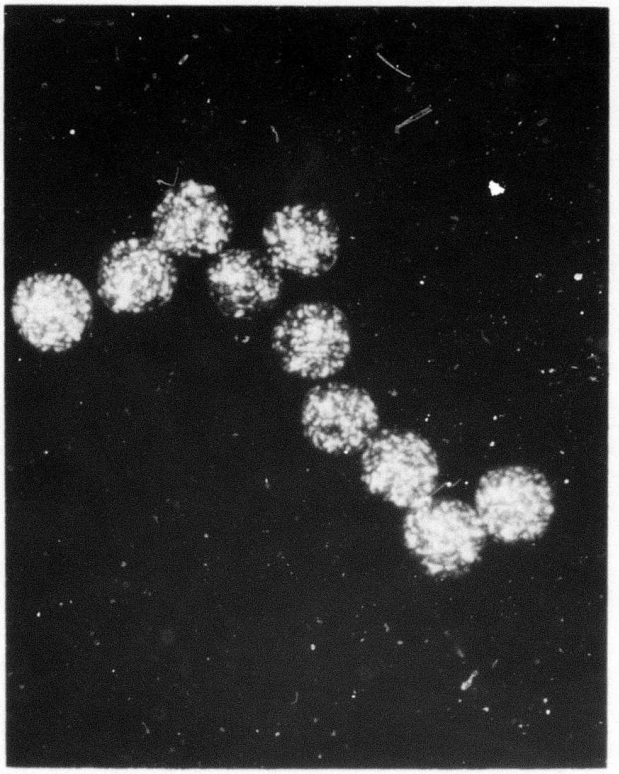

Figure 15. PLM Picture of As-Spun Fibers with Random Structure, Cross Section (1000X)

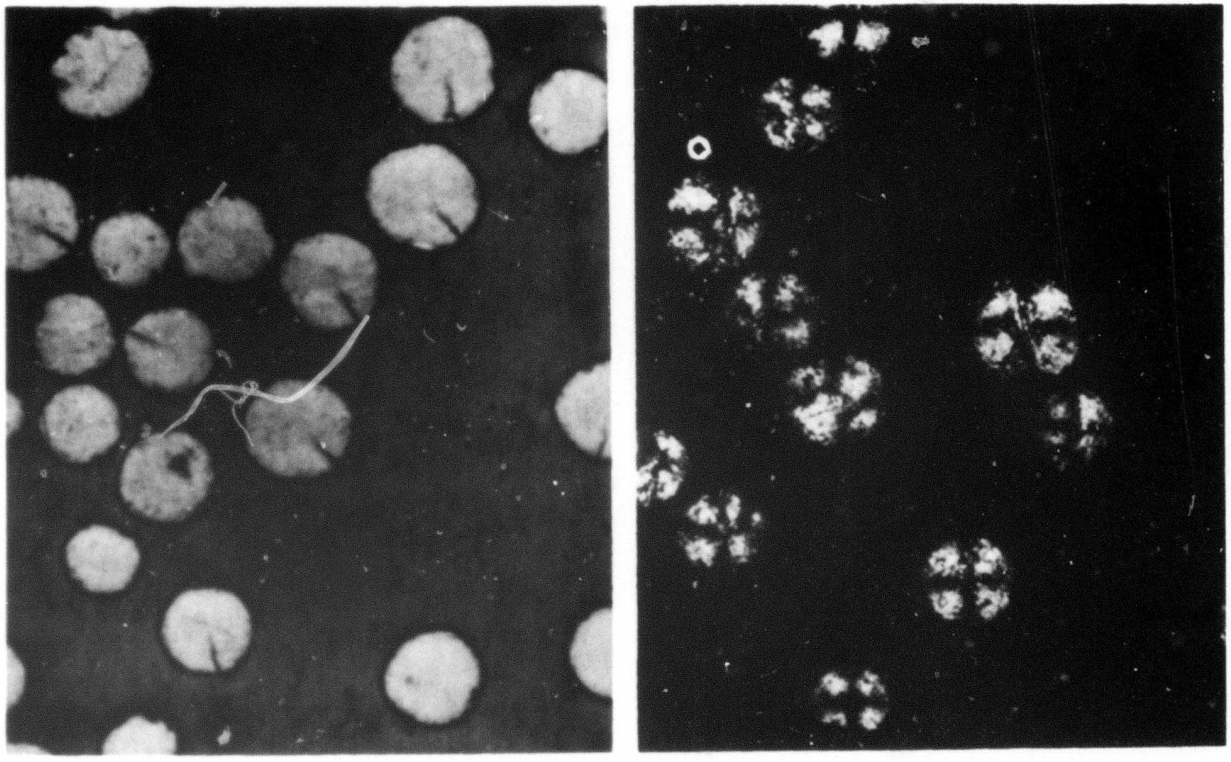

(a) (b)

Figure 16. Micrographs of As-Spun Fibers (1000X)

(a) Cross Section in Bright Field
(b) Cross Section in Polarized Light

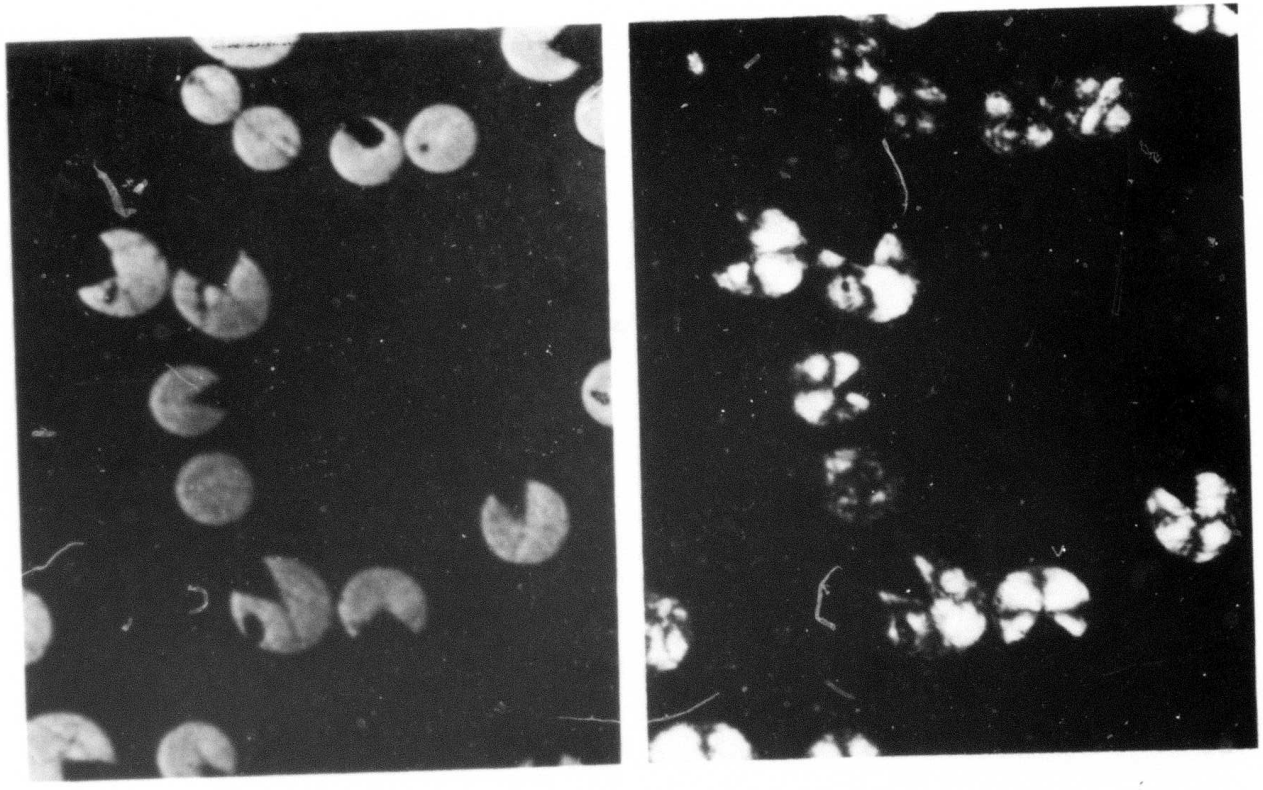

(a) (b)

Figure 17. Micrographs of Fibers with Tensile Strength of 1.55 GPa (225 x 10^3 psi)

(a) Cross Section in Bright Field (1000X)
(b) Cross Section in Polarized Light (1000X)

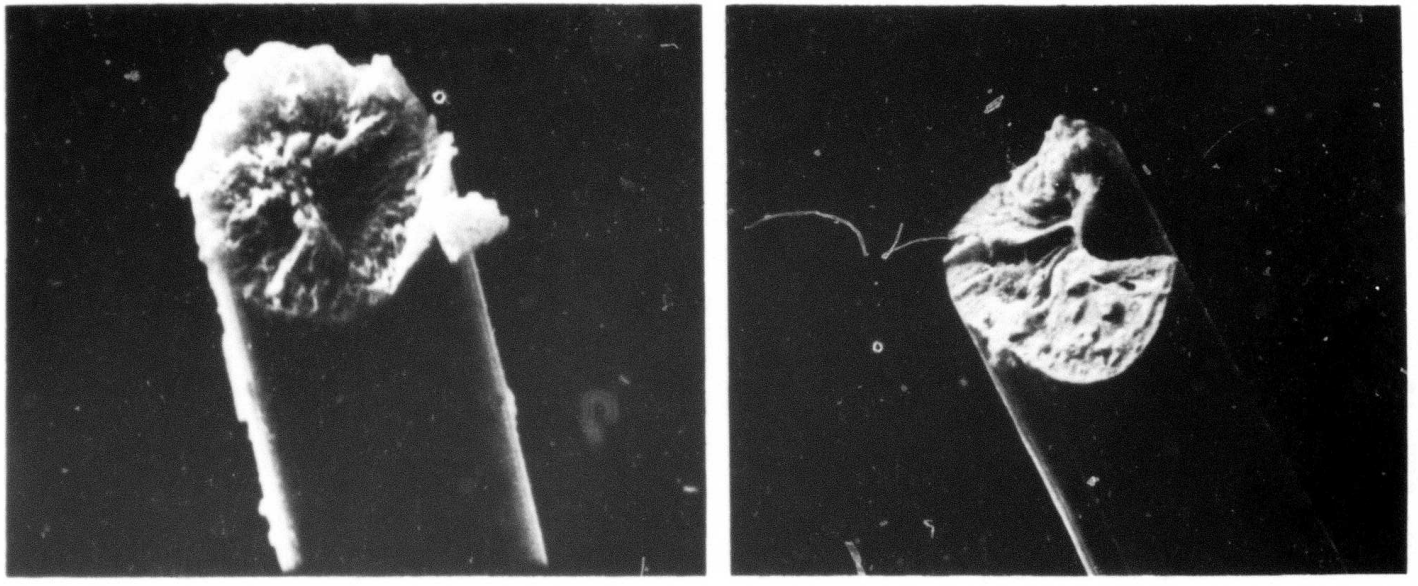

(c)

Figure 17 (Cont'd)

(c) SEM Pictures of Fracture Surfaces
(3000X)

The second sample, which had been given a less extensive thermosetting treatment, had poorer properties after processing to 1650°C; the strand test results were 0.83 GPa (121 x 10^3 psi) for tensile strength and 159 GPa (23 x 10^6 psi) for Young's modulus. The micrographs of this sample are shown in Figure 18. The fibers were obviously underthermoset. There is evidence of a thin, fine-grained skin and a coarse-grained core. This core must have melted completely at some stage of carbonization. The carbonized fibers have also deformed considerably from the original shape of the as-spun fibers.

Since the alteration of the thermosetting conditions significantly changed the structure and resultant properties of the fibers, a second series of samples was studied by optical microscopy to obtain more information on the relationship between structure and thermosetting conditions. The as-spun fibers used in this second study had essentially the same characteristics, including the radial crack, as shown in Figure 16. Five samples were batch processed and subjected to final heat-treatment at 1650°C. The severity of the conditions in the two-step thermosetting process was gradually increased for the samples described in Table XIV. All other processing conditions were kept constant. The single filament test data and the optical microscopy results are given in Table XIV. Optical micrographs of some of these samples are shown in Figures 19 to 21.

Samples A, B, and C were thermoset with increasing residence time in the liquid thermosetting bath, while keeping the gas phase oxidation constant. The main effect was to decrease the fusing together of the filaments. The gas phase treatment increased the viscosity of the entire fiber enough to prevent gross melting in the core but did not make the fibers completely infusible; the fibers had deformed considerably from their original shape.

In Samples D and E, the time of gas phase treatment was quadrupled over that used in Samples A to C. This additional thermosetting was sufficient to make the entire fiber essentially infusible because the original shape was now retained. The structure of Sample E, as determined by optical microscopy, appears to be identical to that of the sample in Figure 17.

Fracture surfaces for the fibers in each of these samples were also examined by scanning electron microscopy. Typical SEM pictures for several of the samples are shown in Figure 22. Figure 22(a) of Sample A shows the fiber deformation during processing. Figure 22(b) of Sample C is a good example of splitting or cracking of a fiber. Figure 22(c) of Sample E indicates that the shape of the cross section has been retained under these thermosetting conditions. The results of the SEM examination are in accord with the optical microscopy results.

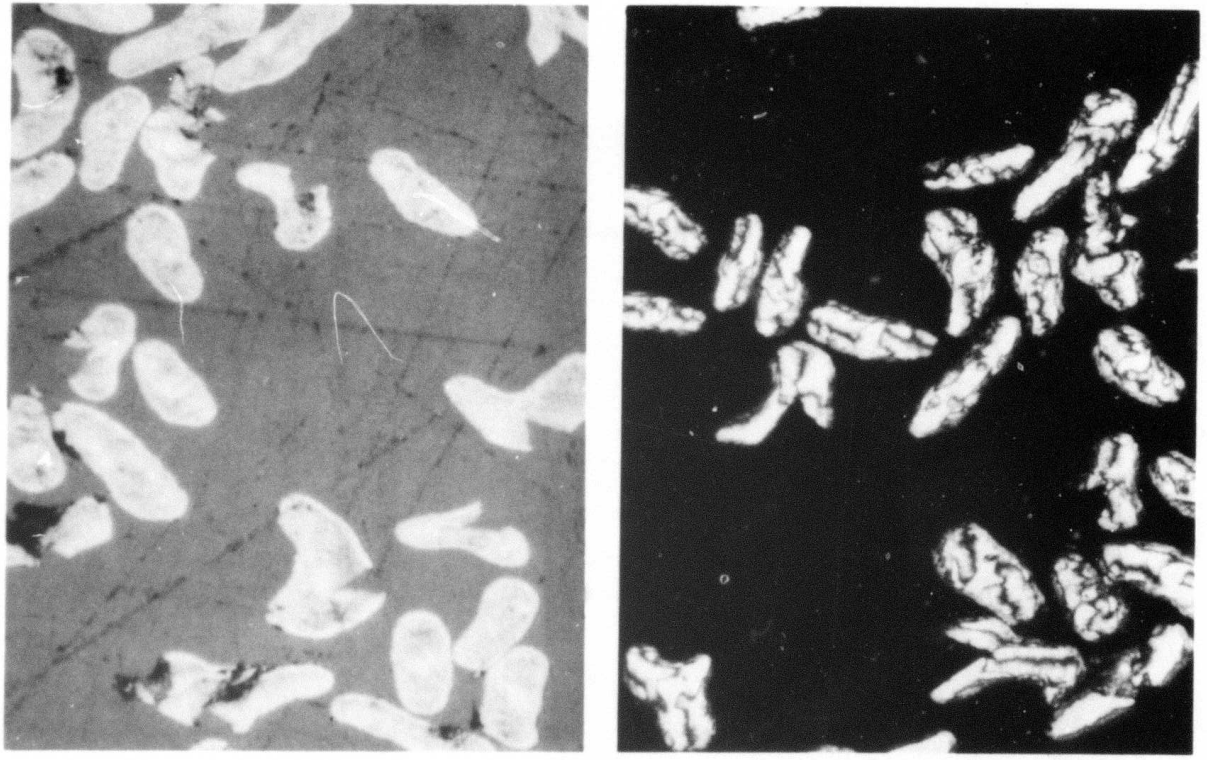

(a) (b)

Figure 18. Micrographs of Fibers with Tensile Strength of 0.83 GPa (121 x 10^3 psi)

(a) Cross Section in Bright Field (1000X)
(b) Cross Section in Polarized Light (1000X)

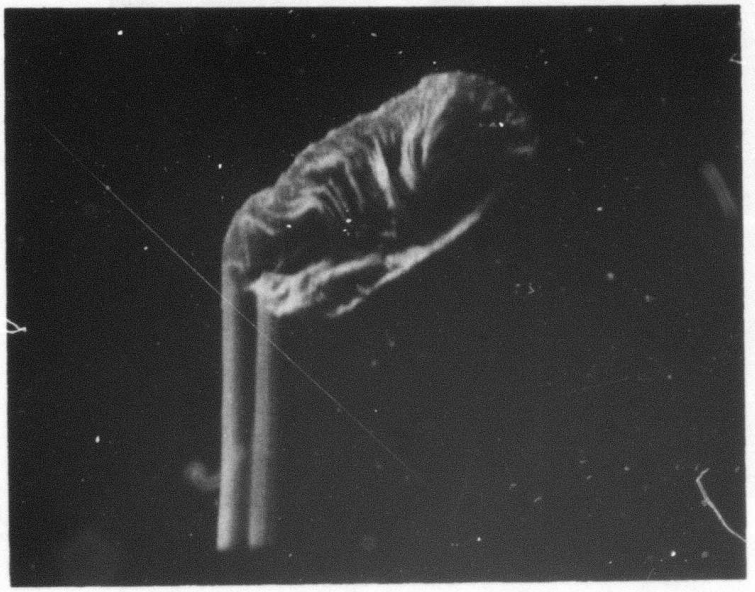

(c)

Figure 18. (Cont'd)
(c) SEM Picture of Fracture Surface (3000X)

TABLE XIV

DEPENDENCE OF FIBER PROPERTIES AND STRUCTURE ON THE SEVERITY OF THERMOSETTING

Sample[a]	Tensile Strength[b] GPa	Tensile Strength[b] psi x 10^{-3}	Young's Modulus GPa	Young's Modulus psi x 10^{-6}	Optical Microscopy Results
A	1.23	178	200	29	Fibers are deformed and some are fused together. Fine-grained domain structure is still present. No skin detectable. Several additional splits and cracks are apparent.
B	1.23	178	165	24	Same as A.
C	1.43	207	214	31	Similar to A and B, except that fibers are not so extensively deformed and fused.
D	1.54	223	241	35	Not much fiber deformation apparent, but many cracks and splits in the fiber are visible.
E	2.23	323	283	41	Original shape of the cross section preserved. No cracks present beyond those attributable to the crack in the as-spun fiber.

[a] All samples batch processed and heat-treated at 1650°C.

[b] Short gauge single filament test.

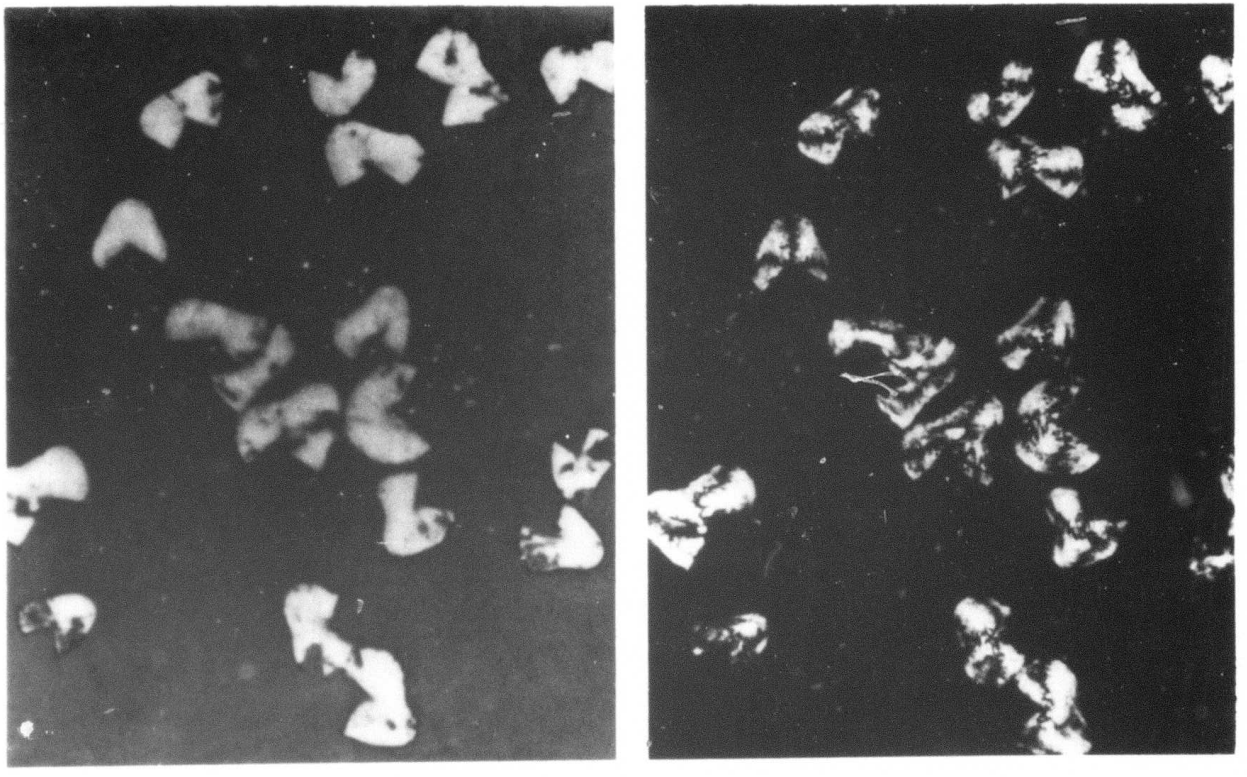

(a) (b)

Figure 19. Micrographs of Sample A in Table XIV. (1000X)

(a) Cross Section in Bright Field
(b) Cross Section in Polarized Light

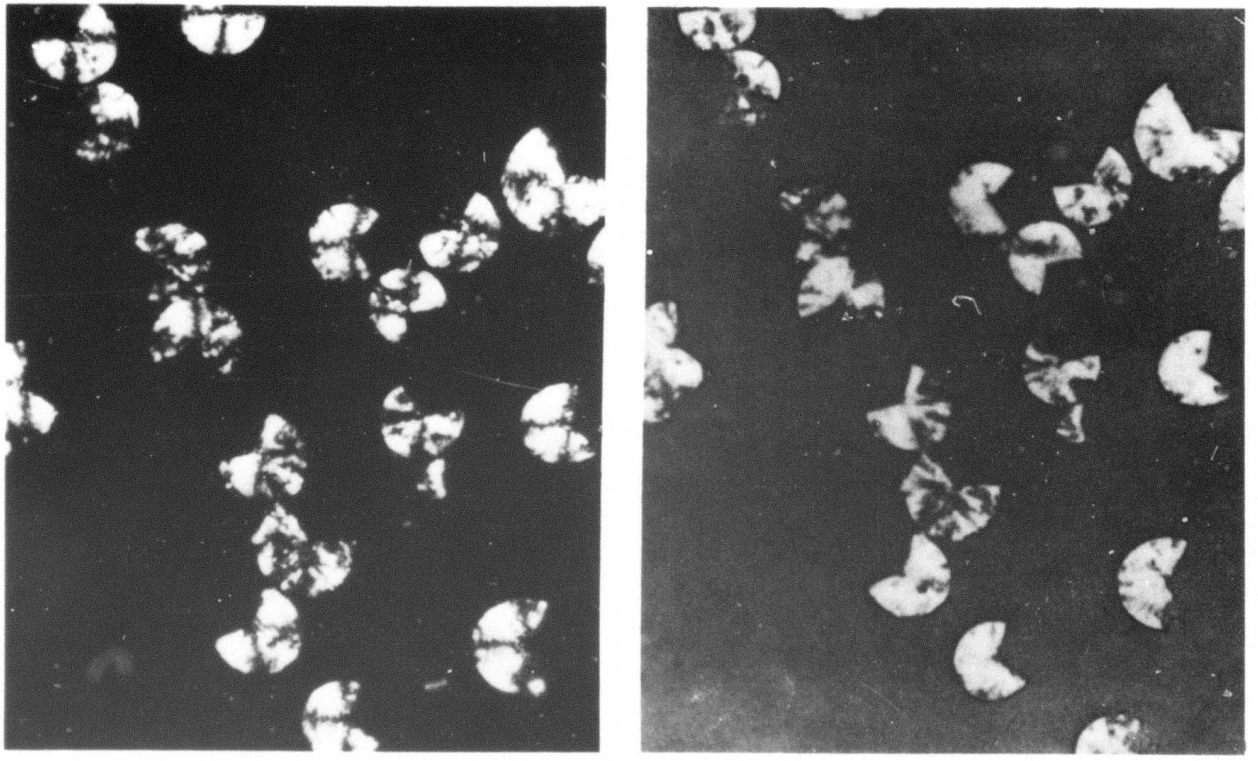

(a) (b)

Figure 20. Micrographs of Sample D in Table XLV (1000X)

(a) Cross Section in Bright Field
(b) Cross Section in Polarized Light

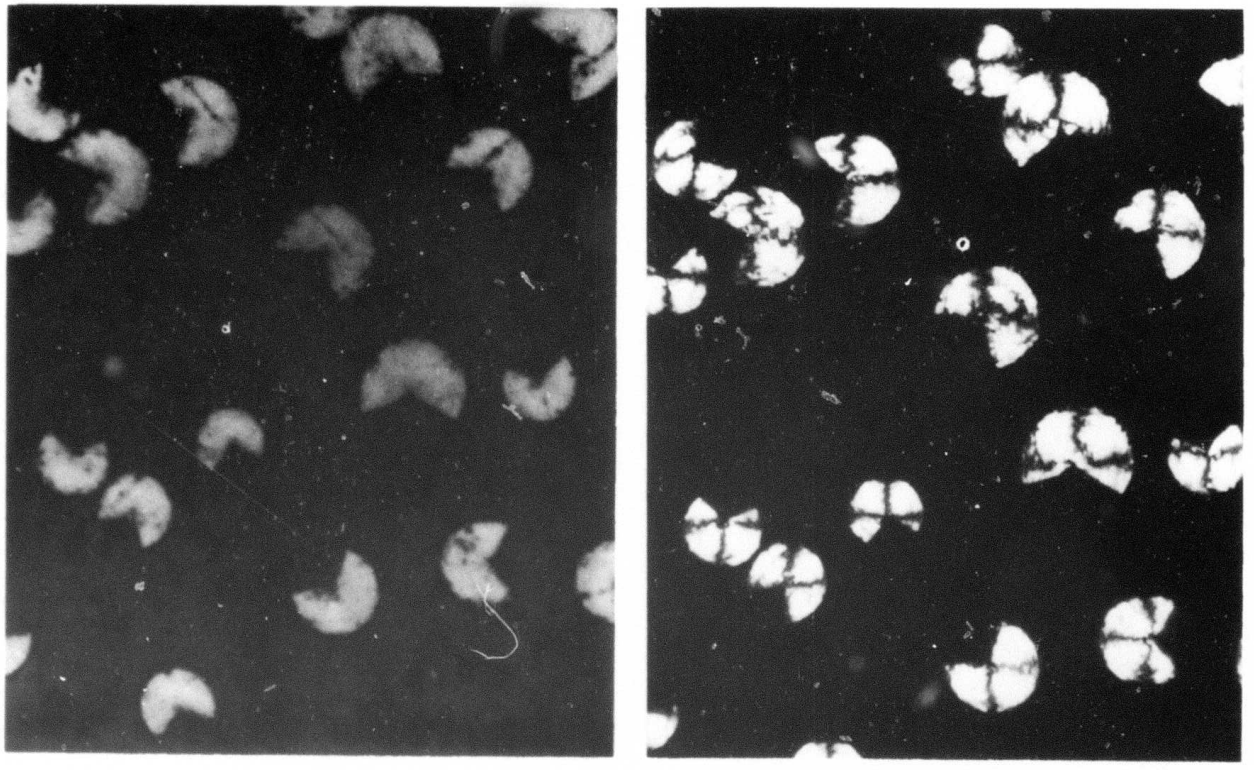

(a) (b)

Figure 21. Micrographs of Sample E in Table XIV (1000X)

(a) Cross Section in Bright Field
(b) Cross Section in Polarized Light

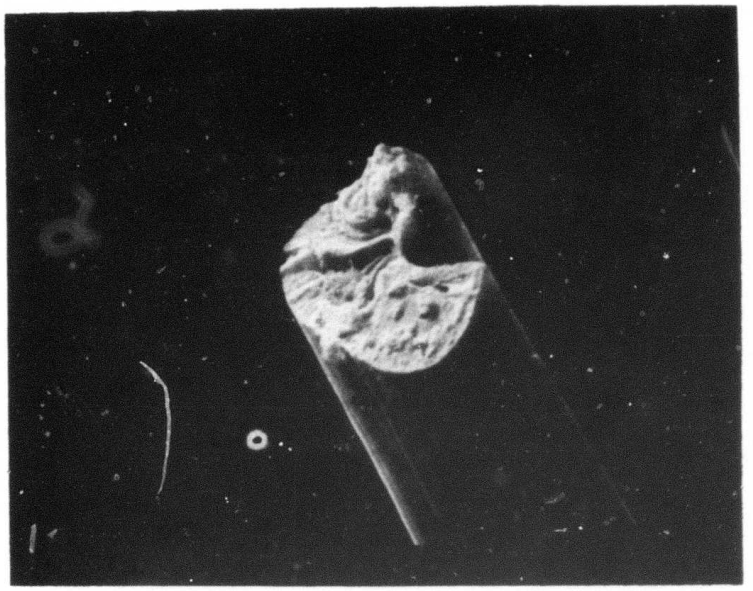

(a)
Sample A

(b)
Sample C

Figure 22. SEM Pictures of Fracture Surfaces of Fibers from Samples Described in Table XIV (3000X)

(c)
Sample E

Figure 22. (Cont'd)

d. Preliminary Results of X-ray Diffraction of Continuously Processed Fibers

The following results were obtained on continuously processed multifilament MP fiber yarn (120 filaments per strand, ~13μm as-spun diameter) as a function of thermosetting and final heat-treatment temperatures. The thermosetting treatments included a liquid bath, air, oxygen, and combinations of these. All the fibers were thermoset and heat-treated continuously at the same rate.

The results are summarized in Table XV. The preferred orientation (FWHM = 30°) and stack height (L_c = 3.4nm) of the as-spun fibers are fairly typical and do not seem to be very dependent upon the pitch or the fiber diameter. The liquid bath thermosetting treatment, since it predominantly affects the surface of the fiber, produced no changes in these bulk X-ray parameters. Gas phase oxidation of the fibers, either with or without prior liquid bath treatment, decreased both the degree of preferred orientation and the crystalline stack height. Unfortunately, it is not clear from samples number 3 and 4 in Table XV whether the increase in disorder occurred from the oxidative cross linking or the subsequent heat-treatment. As can be seen from the samples numbered 5 to 10, the degree of preferred orientation present after the initial thermosetting partially recovered upon further heat-treatment to 700°C, while the crystalline stack height continued to decrease. Both the degree of preferred orientation and L_c began to increase at some temperature between 1000° and 1650°C.

e. Extended Study of Continuously Processed Fibers

The first correlations of thermosetting condition and fiber structure with the fiber properties in multifilament yarn were described in Section c. The best properties were obtained when the thermosetting conditions were at least sufficient to preserve the fine-grained domains and the undeformed shape of the as-spun fiber. A more extensive study was undertaken in which an as-spun multifilament yarn was continuously processed to 1700°C after 16 different thermosetting conditions. These thermosetting conditions varied from the relatively mold ones used for the samples in Table XIV of Section c to conditions which were at least an order of magnitude more severe. Selected carbonized fiber samples were examined by X-ray diffraction, optical microscopy, and SEM.

In spite of the wide variation in thermosetting treatments, the preferred orientation (FWHM) and crystalline stack height (L_c) were independent of these treatments, namely, 21.6 ± 0.5° and 6.1 ± 0.3nm, respectively. Similarly, the optical microscopy and SEM revealed identical features to those described in Table XIV for all samples subjected to comparable thermosetting conditions, confirming the reproducibility of the processing.

TABLE XV

X-RAY STRUCTURAL PARAMETERS FOR CONTINUOUSLY PROCESSED MP PITCH FIBERS

Sample Number	Thermosetting Media	Final Heat-Treatment Temp. in Nitrogen (°C)	Preferred Orientation FWHM (°)	Crystalline Stack Height L_c (nm)
1	None (as-spun)	---	30	3.4
2	Liquid Bath Only	---	29	3.3
3	Liquid Bath + Oxygen	---	36	2.6
4	Air + Oxygen	---	40	1.7
5	Same as No. 3	700	32	1.4
6	" " " "	1000	32	1.6
7	" " " "	1650	16	7.1
8	Same as No. 4	700	31	1.5
9	" " " "	1000	31	1.8
10	" " " "	1650	21	4.7

The elastic modulus was somewhat lower in the samples which were thermoset as Sample B in Table XIV, that is, under the mild conditions which resulted in a slight deformation of the fiber cross section. The modulus was higher for more severely thermoset samples comparable to Sample E in Table XIV. While the trend for the elastic modulus was the same as in Table XIV, a corresponding increase in strength with increasing thermosetting severity did not occur. For the samples which were thermoset much more severely than those of Sample E in Table XIV, there was no definite indication of further change in elastic modulus or tensile strength. It is not yet clear why the trend of increasing elastic moduli for the fibers thermoset under milder conditions, comparable to those used for the samples in Table XIV, was not reflected in the X-ray preferred orientation. For those samples in which the severity of the thermosetting was equal to or greater than that employed in Sample E of Table XIV, there was no discernible difference in the appearance of the fibers examined either by optical microscopy or by SEM. This result is in accord with the X-ray diffraction data and the fiber property data, which also do not indicate any appreciable changes. Apparently, increasing the severity of the thermosetting conditions an order of magnitude beyond that necessary to preserve the fine-grained domain structure and prevent deformation does not lead to any dramatic change in structure or properties for the multifilament yarn used in this investigation.

Many fracture surfaces of more severely thermoset fibers described above were examined by SEM. The most common type of fracture is shown in Figure 23(a). This fracture surface is similar to those shown in Figures 17(c) and 22(c). Less common types of fracture surface are shown in Figure 23(b), (c), and (d). Figure 23(b) shows what is apparently a "fibril" protruding from the surface. Figure 23(c) shows a surface in which portions of the fracture occurred in two different planes perpendicular to the fiber axis. Figure 23(d) shows a surface where the intersection of the outer fiber surface and fracture surface forms a helix. Fracture surfaces with voids have not been observed, and no obvious surface flaws have been found with the possible exception of fractures such as that shown in Figure 23(d). The major gross defect for this type of these particular carbonized fibers is the "missing wedge," which has its origin in the radial crack in the as-spun fiber.

f. Preliminary Transmission Electron Microscopy Observations (TEM)

Transmission electron microscopy studies using the JEM-6A microscope have been initiated to determine the microstructural details of MP carbon fibers at all stages of processing. The efforts to date have been aimed at finding the methods and techniques which best reveal the structural details.

A sample of adequately thermoset, carbonized (1650°C) MP fibers has been used. Thin longitudinal and transverse sections were prepared by microtoming fibers encapsulated in a mixture of methyl and butyl methacrylate.

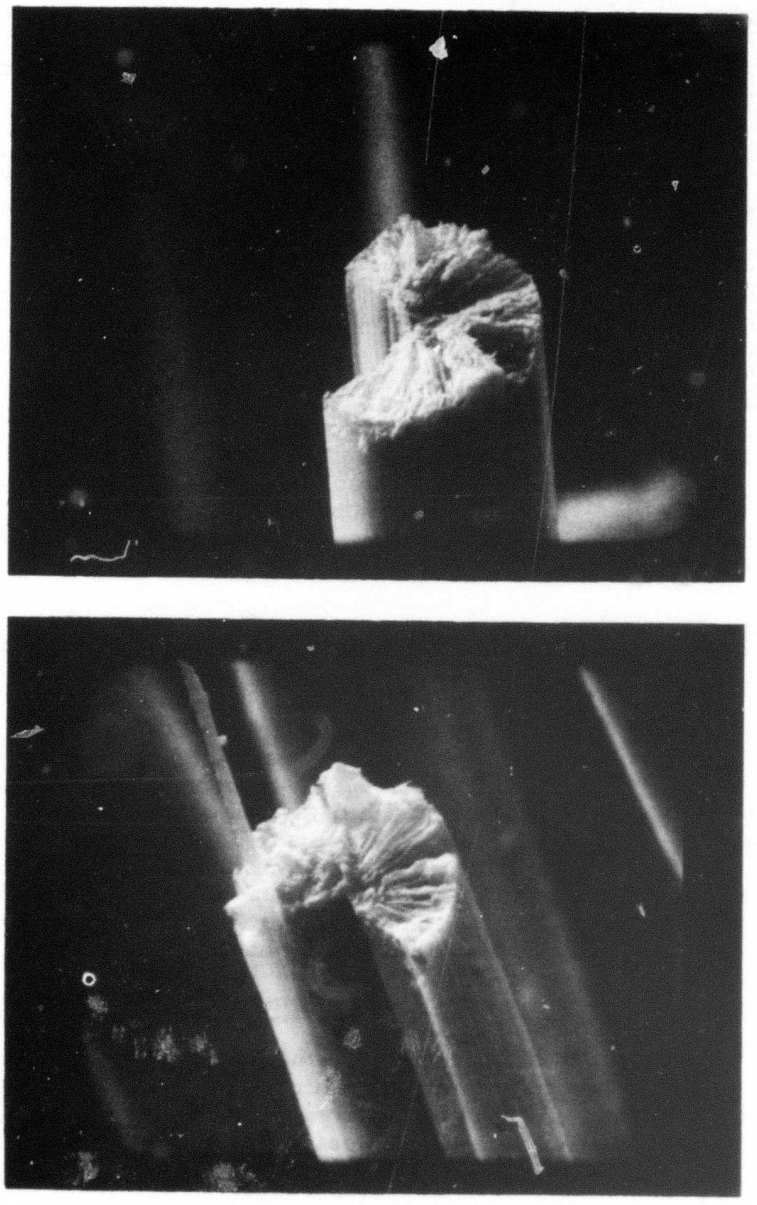

(a)

(b)

Figure 23. SEM Pictures of Carbonized Fibers (3000X)

(a) Typical Fracture Surface
(b) Fracture Surfaces with "Fibril"

(c)

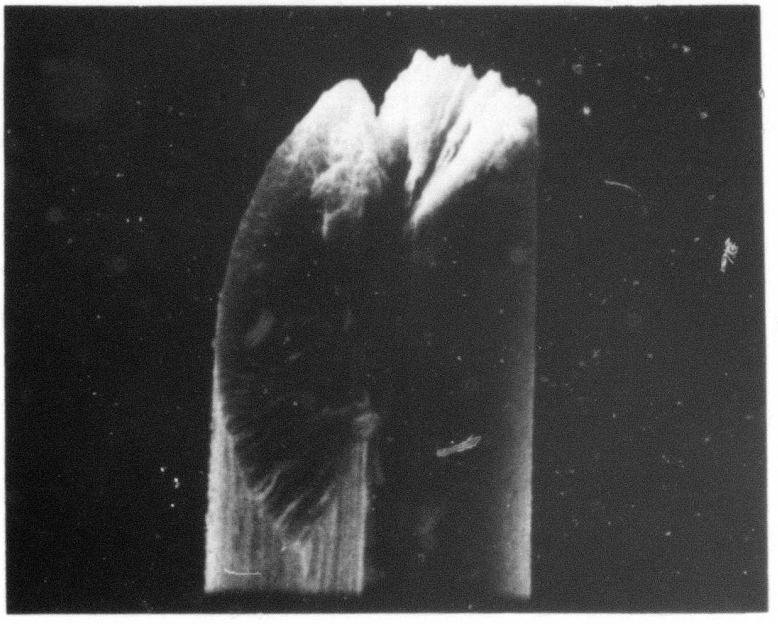

(d)

Figure 23. (Cont'd)

(c) One Type of Less Common Fracture Surface
(d) "Helix" Type of Fracture Surface

The transverse sections were very poor because the fibers fractured too easily in the axial direction. Some reasonably intact longitudinal sections of the portion of the fiber close to the surface were obtained. An example of a bright field micrograph and selected area electron diffraction patterns obtained from a longitudinal section is shown in Figure 24. The electron diffraction pattern indicates that the layer planes are oriented along the fiber axis, which is in agreement with the polarized light and X-ray diffraction results. It is not clear yet whether the striations parallel to the fiber edge in Figure 24 reflect the structure of the carbon fiber or are an artifact produced by the sectioning.

Pieces of crushed carbonized fibers were also examined in bright field and by selected area electron diffraction. The chips appear to be thin, elongated platelets which are similar in appearance to the longitudinal slices. A bright field micrograph and the selected area electron diffraction pattern, obtained from a piece of crushed fiber, are shown in Figure 25. The orientation determined by the electron diffraction pattern shows that the long direction of the chip was parallel to the fiber axis.

A sample of MP fibers, which had a radial layer plane orientation as determined by PLM, was examined in thin sections in both the as-spun and partially processed state (500°C). Thin longitudinal and transverse sections were obtained for the as-spun fibers, but the damage from the microtoming was considerable. Weak selected area electron diffraction patterns, indicating preferential orientation, were observable on the phosphor screen of the microscope in some of the sections, but the damage to the sample, probably from melting in the electron beam was too rapid to allow adequate photography of the diffraction patterns. Visual observation of the transitory diffraction patterns indicated that the layer plane was along the fiber axis in the longitudinal slices and radial in the transverse slice (cross section). Thin longitudinal and transverse sections were also obtained for the 500°C fiber. These sections were also damaged considerably by the microtoming. The weak electron diffraction patterns, which were observed in some but not all sections of this sample, were considerably more persistent, presumably because of the better thermal stability of the 500°C fiber. The layer plane orientation was again along the fiber axis in the longitudinal sections, and radial in the transverse slices (cross section).

The results for preferred orientation in the axial and transverse directions obtained so far by electron diffraction in the TEM are in accord with the PLM results described earlier. In addition, no evidence of any micropores, resembling those observed in carbon fibers derived from PAN has been detected yet. Much more effort will be required to utilize TEM techniques in the study of MP carbon fiber structure.

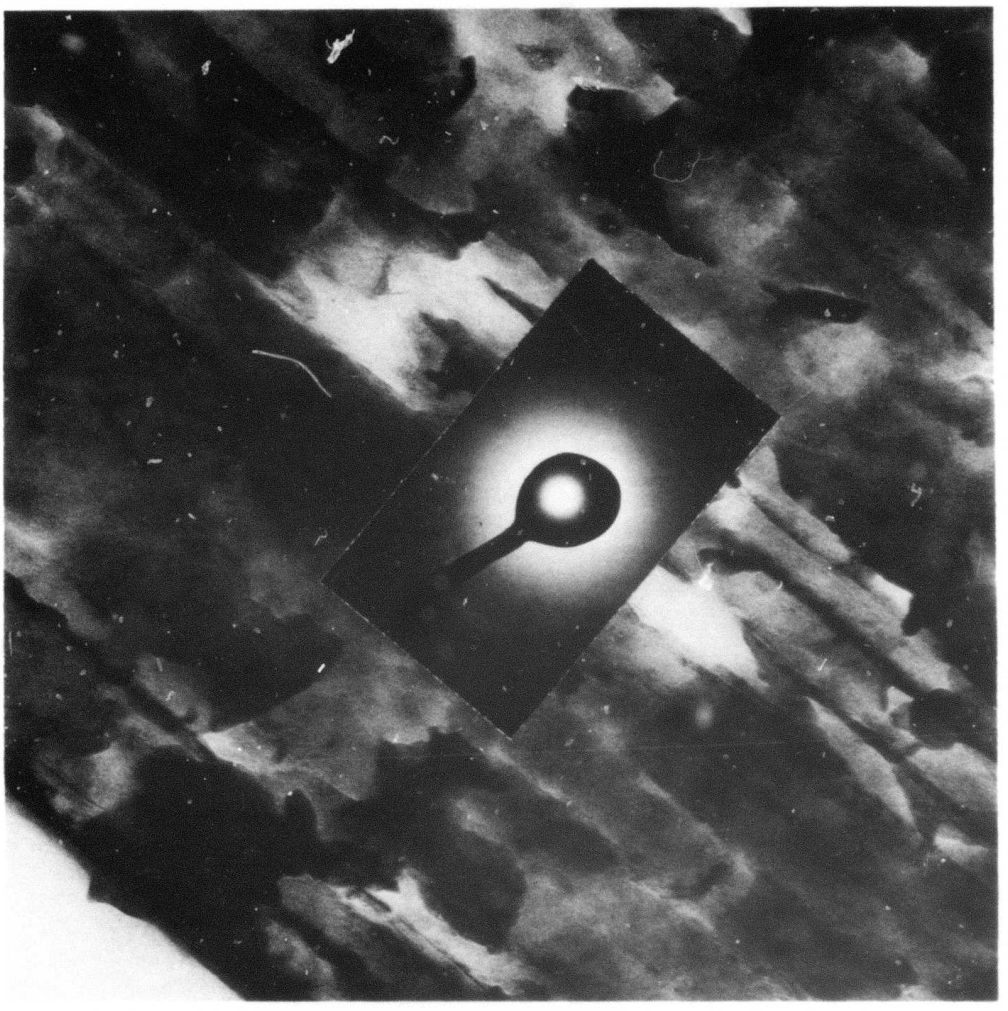

Figure 24. TEM Bright Field Micrograph and d_{002} Selected Area Electron Diffraction Pattern for a Longitudinal Slice of a Carbonized Fiber. Fiber edge is at lower left. Magnification is 35,600X.

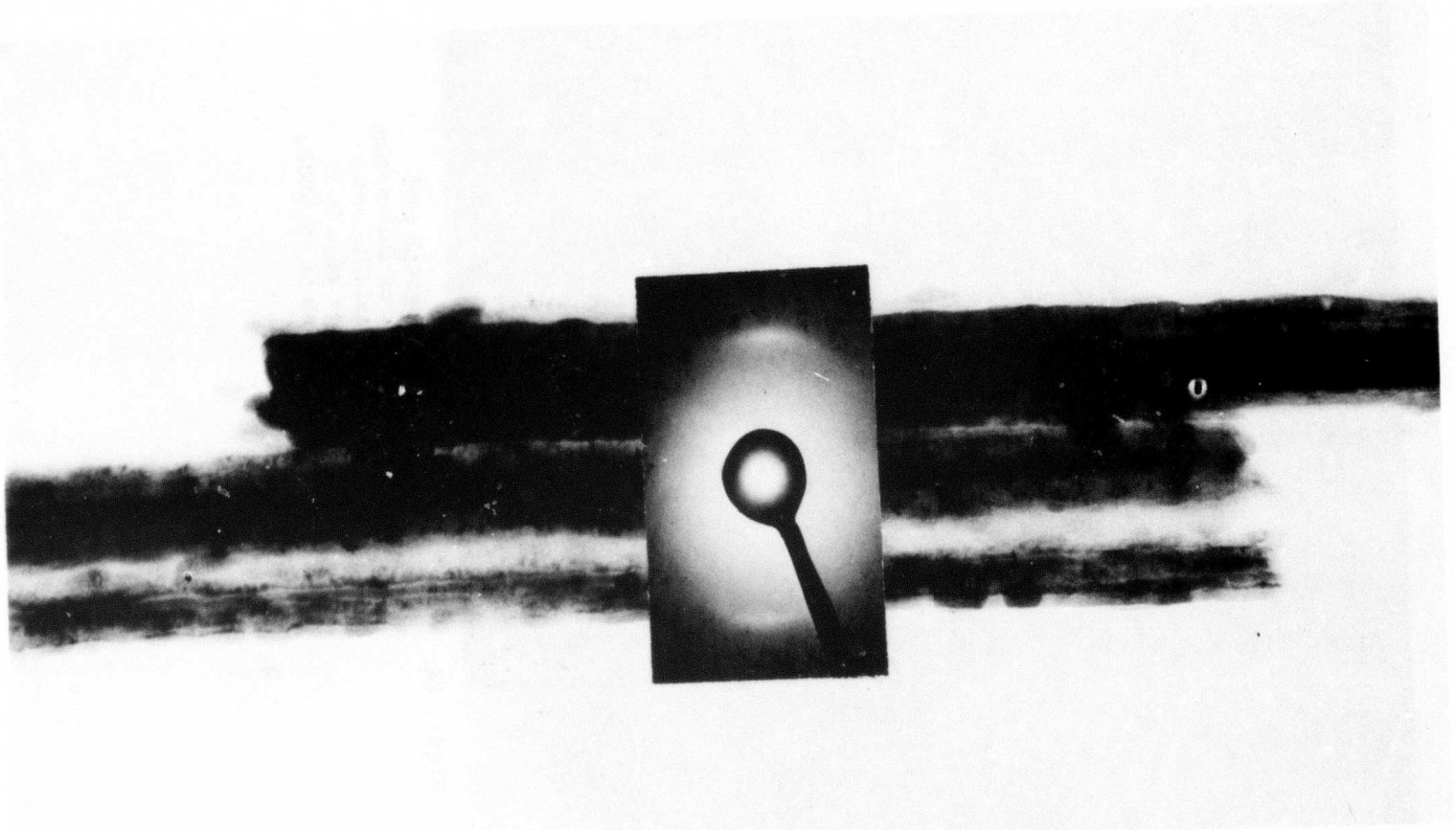

Figure 25. TEM Bright Field Micrograph and d_{002} Selected Area Electron Diffraction Pattern from a Piece of Crushed Fiber. Magnification is 35,600X.

SECTION IX

COMPOSITE SHEAR STRENGTH

The torsional shear strength of an epoxy composite with carbon fibers from MP pitch was determined to be only 32.8 MPa (4750 psi). The fiber used in this test was processed to 1650°C and possessed a short gauge tensile strength of 1.83 GPa (265 x 10^3 psi) and a Young's modulus of 172 GPa (25 x 10^6 psi). However, the fiber responded readily to a surface treatment. The treated fiber exhibited a composite shear strength of 89.0 MPa (12,900 psi). Fiber loading in the torsional shear rod was 50 percent by volume in an ERL 2256 epoxy matrix.

REFERENCES

(1) Union Carbide Corporation, "Graphite Fibers from Pitch," Technical Report AFML-TR-73-174, Part I (June 1973), p. 15.

(2) T. Edstrom and B. A. Petro, J. Poly. Sci., Pt. C, 177, (No. 21, 1968).

(3) Ref. 1., p. 9.

(4) T. Araki, et al. "Infusibilization Treatment of Pitch Articles," British Patent No. 1307392, 21 Feb. 1973.

(5) Ref. 1, p. 34.

(6) R. H. Kribbs, J. of Micro. 94, 273 (1971).

(7) Ref. 1., p. 38.

*U.S.Government Printing Office: 1974 — 657-016/268